Dorsal Column Stimulation for Therapy, Artificial Somatosensation and Cortico-Spinal Communication

by

Amol P. Yadav

Department of Biomedical Engineering
Duke University

Date:_____

Approved:

_____
Miguel A.L. Nicolelis, Co-Chair

_____
Craig Henriquez, Co-Chair

_____
Marc Sommer

_____
Loren Nolte

_____
Kafui Dzirasa

Dissertation submitted in partial fulfillment of the requirements for the degree of
Doctor of Philosophy in the Department of Biomedical Engineering
in the Graduate School of Duke University
2015

ABSTRACT

Dorsal Column Stimulation for Therapy, Artificial Somatosensation and Cortico-Spinal Communication

by

Amol P. Yadav

Department of Biomedical Engineering
Duke University

Date:_____

Approved:

_____
Miguel A.L. Nicolelis, Co-Chair

_____
Craig Henriquez

_____
Marc Sommer

_____
Loren Nolte

_____
Kafui Dzirasa

An abstract of a dissertation submitted in partial fulfillment of the requirements for the degree of Doctor of Philosophy in the Department of Biomedical Engineering in the Graduate School of Duke University
2015

Copyright by
Amol P. Yadav
2015

Abstract

The spinal cord is an information highway continuously transmitting afferent and efferent signals to and from the brain. Although spinal cord stimulation has been used for the treatment of chronic pain for decades, its potential has not been fully explored. Spinal cord stimulation has never been used with the aim to transmit relevant information to the brain. Although, various locations along the sensory pathway have been explored for generating electrical stimulation induced sensory percepts, right from peripheral nerves, to thalamus to primary somatosensory cortex, the role of spinal cord has been largely neglected. In this dissertation, I have attempted to investigate if, electrical stimulation of dorsal columns of spinal cord called as Dorsal Column Stimulation (DCS) can be used as an effective technique to communicate therapeutic and somatosensory information to the brain.

To study the long term effects of DCS, I employed the 6-hydroxydopamine (6-OHDA) rodent model of Parkinson's Disease (PD). Twice a week DCS for 30 minutes resulted in a dramatic recovery of weight and behavioral symptoms in rats treated with striatal infusions of 6-OHDA. The improvement in motor symptoms was accompanied by higher dopaminergic innervation in the striatum and increased cell count of dopaminergic neurons in the substantia nigra pars compacta (SNc). These results suggest that DCS has a chronic therapeutic and neuroprotective effect, increasing its potential as a new clinical option for treating PD patients. Thus, I was able to demonstrate the long-term efficacy of DCS, as a technique for therapeutic intervention.

Subsequently, I investigated if DCS can be used as a technique to transmit artificial somatosensory information to the cortex and trained rats to discriminate multiple artificial tactile sensations. Rats were able to successfully differentiate 4 different tactile percepts generated by varying temporal patterns of DCS. As the rats learnt the task, significant changes in the encoding of this artificial information were observed in multiple brain areas. Finally, I created a Brainet that interconnected two rats: an encoder and a decoder, whereby, cortical signals from the encoder rat were processed by a neural decoder while it performed a tactile discrimination task and transmitted to the spinal cord of the decoder using DCS. My study demonstrated for the first time, a cortico-spinal communication between different organisms.

My obtained results suggest that DCS, a semi-invasive technique, can be used in the future to send prosthetic somatosensory information to the brain or to enable a healthy brain to directly modulate neural activity in the nervous system of a patient, facilitating plasticity mechanism needed for efficient recovery.

To the yogis and mystics of India who learnt to use their mind as a tool to transcend the limits of human sensory perception.

Contents

List of Figures

List of Abbreviations

6-OHDA	6-hydroxydopamine
ANOVA	Analysis of Variance
BDNF	Brain Derived Neurotropic Factor
BG	Basal Ganglia
BTBI	Brain To Brain Interface
CPU	Caudate Putamen
CSF	Cerebrospinal Fluid
CST	Corticospinal Tract
DA	Dopamine
DBS	Deep Brain Stimulation
DC	Dorsal Column
DCS	Dorsal Column Stimulation
DR	Dorsal Root
EEG	Electroencephalography
GDNF	Glail Derived Nerve Growth Factor
GPi	Globus Pallidus Internal
ICMS	Intracortical Microstimulation
IHC	Immunohistochemistry
L-dopa	Levodopa
LID	Levodopa Induced Dyskinesia

M1	Primary motor cortex
MPTP	1-methyl-4-phenyl-1,2,3,6-tetrahydropyridine
MSNs	Medium Spiny Neurons
PD	Parkinson's Disease
S1	Primary somatosensory cortex
SCS	Spinal Cord Stimulation
SNc	Substantia nigra pars compacta
STN	Subthalamic nucleus
STR	Striatum
T2	Second thoracic vertebra
T3	Third thoracic vertebra
TH	Tyrosine hydroxylase
TH-IR	Tyrosine hydroxylase Immunoreactive
TMS	Transcranial Magnetic Stimulation
UPDRS	Unified Parkinson's Disease Rating Scale

Acknowledgements

My greatest gratitude is reserved for my parents for their constant support and encouragement throughout my course of study. Had they not put their trust and belief in me while I went through this unpredictable journey, I would have never reached this stage.

Secondly, I would like to thank Craig Henriquez, Miguel Nicolelis and Loren Nolte who were extremely generous in their letter of recommendations when I applied for the PhD program at Duke. They have guided me along my way and it is my deep honor that I will defend my dissertation in their presence as they serve on my PhD committee. I am also thankful to Kafui Dzirasa and Marc Sommer for providing important inputs and suggestions during my course of study and serving on my committee. Most importantly, I would not have made it here without the timely guidance provided by my advisor Miguel Nicolelis. He has been very kind to give me ample freedom to explore interesting research avenues and also provide necessary advice if I ventured too far.

I also owe a lot of gratitude to post-docs in our group, namely Romulo Fuentes, Hao Zhang, Miguel Pais-Vieira and Eric Thomson for teaching me all the research skills required to finish this dissertation. Romulo has been a dear friend and mentor who taught me spinal electrode fabrication and implantation methods, various analyses and grant writing. Miguel Pais-Vieira happens to be the person I would run to every time I had questions about electrophysiology and data presentation. He has been an excellent role model in teaching me how to design experiments and finish them in a well-timed manner.

I would also like to thank the numerous undergraduate and exchange students that I had the pleasure to work with. They have been instrumental in helping me with my experiments, specially, Thais Vinholo, Click Wang, Cindy Choi, Daniel Li, John Scott, Haley Talbot and Chelsea Liu. Although, I set out to mentor them, I ended up learning a lot of things from them.

My dissertation would not have been complete without the administrative support of Laura Oliveira, Susan Halkiotis, Terry Jones and the technical expertise of Gary Lehew and Jim Meloy. I reserve my sincere gratitude for their encouraging support.

Finally, I would like to thank Sophie Koroloff for her constant support and encouragement throughout my PhD. Her proofreading abilities, patience and honest criticism while I practiced various presentations and speeches have been instrumental in shaping my public speaking and presentations skills.

1. Introduction

In this dissertation I have demonstrated the use of electrical stimulation of the dorsal columns of the spinal cord, referred to as Dorsal Column Stimulation (DCS) as a technique to transmit both therapeutic as well as somatosensory information to the brain. Initially, to test the long term therapeutic benefits of DCS, I used an animal model of Parkinson's Disease and studied the chronic effects of DCS on the functional and structural recovery of the dopaminergic system. Later, I investigated the ability of animals to discriminate multiple artificial tactile sensations generated by varying patterns of DCS. Then, to solidify my claim that DCS can be used to communicate with the brain, I developed a real-time cortico-spinal interface for the transfer of real as well as artificial tactile information between two animals using DCS to encode data and neuronal signals to decode it.

The spinal cord serves as the information highway transmitting non-noxious as well as nociceptive sensory information from various parts of the body to supra-spinal structures in the brain. Although, spinal cord stimulation has been used for the treatment of chronic pain for more than four decades, its full potential as a channel to transmit information to the brain has not been fully explored. In this chapter I will go through a brief literature review that led me to explore the potential of dorsal column stimulation as a channel for therapeutic intervention and communication with the brain, followed by a description of how the chapters are organized.

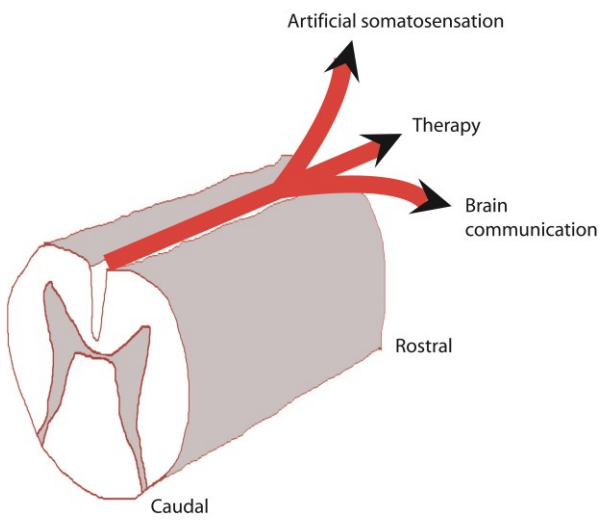

Figure 1.1 Schematic of dorsal surface of spinal cord to be used as a channel for artificial somatosensation, therapy and brain communication

1.1 Spinal Cord Stimulation

Spinal cord stimulation (SCS) was first used for the treatment of chronic pain by Dr. Shealy and coworkers at Case Western Reserve University in 1967 (Shealy *et al.*, 1967) . Since then, it has been used for the last 4 decades, for the treatment of different pain syndromes. Initially, the gate control theory proposed by (Melzack & Wall, 1965), that, activation of large diameter 'Aβ' fibers carrying tactile information and suppression of noxious 'C' fibers carrying pain signals, in the dorsal horn, by SCS, formed the basis for relief from chronic pain, but, subsequently various mechanisms underlying pain relief have been uncovered, namely, effect of paresthesia and activation of supraspinal circuits produced by orthodromic activation of dorsal columns or, changes in the local transmitter systems and suppression of dorsal horn neurons in the case of neuropathic pain or,

balancing of oxygen supply and demand by inhibition of sympathetic activity in the case of ischemic pain (Linderoth & Foreman, 1999; D'Mello & Dickenson, 2008).

Computational modelling studies have shown that, epidural SCS applied within the therapeutic range, usually activates dorsal column (DC) fibers, restricted to a depth of 0.2-0.25mm from the surface and the dorsal roots (DR), in the vicinity of the stimulating cathode, which is responsible for the paresthesia effect experienced by patients (Holsheimer, 2002). However, the probability of paresthesia as a function of rostrocaudal cathode position, is related to the ratio of DC and DR fiber thresholds, which varies along the vertebral column, depending on the thickness of the Cerebrospinal Fluid (CSF) layer (Holsheimer & Barolat, 1998).

Recent work in our laboratory on the use of DCS for Parkinson's Disease (PD) has shown that, DCS can be used to activate afferent dorsal column fibers, to interfere with pathological corticostriatal neuronal activity associated with PD (Fuentes *et al.*, 2009). Also, it has been demonstrated that, DCS can result in remodeling of corticospinal projections, to aid in partial recovery of locomotion, in spinal cord injured rats (van den Brand *et al.*, 2012). While, functional magnetic resonance imaging of cortical structures during DCS application revealed clear modulation of cortical structures (Stancak *et al.*, 2008), DCS is also known to cause changes in gene expression in supraspinal structures, which in turn may lead to long-term sustained effects (Dejongste *et al.*, 1998; Maeda *et al.*, 2009).

1.2 Parkinson's Disease

Parkinson's disease (PD) is a chronic debilitating neurodegenerative disorder with no cure caused by progressive loss of the dopaminergic neurons of the nigrostriatal pathway (Carlsson, 1972). Administration of L-dopa, a pharmacological intervention, for a long time, is known to result in fluctuations in clinical response and L-dopa induced dyskinesia (LID) (Nagatsua & Sawadab, 2009). Although, Deep Brain Stimulation (DBS), a therapeutic approach involving electrical stimulation of subcortical structures, is very effective in alleviating the motor symptoms of PD best candidates for this treatment are idiopathic PD patients with motor fluctuations and LID (Benabid, 2003) and based on current criteria for candidate selection (Pizzolato & Mandat, 2012), only 1.6 to 4.5% of the PD patients are eligible for DBS (Morgante *et al.*, 2007).

1.2.1 Role of Basal Ganglia in PD

The basal ganglia (BG) are a group of subcortical nuclei that contribute to the generation of goal-directed behavior by integrating sensory, cognitive and executive information. BG works in concert with the cortex to orchestrate and execute planned, motivated behaviors that require motor, cognitive and limbic circuits (Haber, 2003). Regions within the basal ganglia are anatomically and physiologically associated with each of these functional circuits. The dorsolateral portion of the striatum - the input structure of BG is associated with the control of movement. Hence, diseases affecting motor control are linked with the pathology of the basal ganglia. Substantia nigra pars compacta (SNc) sends dopaminergic projections to the medium spiny neurons (MSNs) in the striatum to modulate the activity of the basal ganglia by exciting MSNs projecting in the direct

pathway and inhibiting those that project in the indirect pathway. Degeneration of the nigrostriatal dopaminergic system due to loss of dopaminergic neurons of the SNc and subsequent dopamine deficiency in the striatum are common findings in postmortem studies of PD patients (Kish *et al.*, 1988; Fahn, 2003). Thus most motor symptoms of PD can be attributed to the imbalance of activity in the direct/indirect pathways, (increased activity in indirect pathway/decreased activity in direct pathway) due to destruction of dopaminergic projections from the SNc to the striatum. Since the dopaminergic projection from SNc to the striatum seems to be important for the initiation and execution of movement, several methods that either directly or indirectly reduce the amount of striatal dopamine in animal models [namely; using 6-hydroxydopamine (6-OHDA) (Mendez & Finn, 1975) or 1-methyl-4-phenyl-1,2,3,6-tetrahydropyridine (MPTP) (Burns *et al.*, 1983) for chemical lesioning of dopaminergic neurons; transgenic or viral vector-induced overexpression of α-synuclein (Kirik *et al.*, 2002); severe inhibition of dopamine synthesis (Costa *et al.*, 2006); genetically targeted dopaminergic mitochondrial injury (Ekstrand *et al.*, 2007) have been successful in replicating some of the cardinal symptoms like hypokinesia and rigidity observed in PD patients.

1.2.2 6-OHDA rat model

The 6-OHDA rat model is one of the most widely used animal models for studying PD. Different 6-OHDA rat models have been developed in which the neurotoxin is injected into different parts of the nigrostriatal pathway: the medial forebrain bundle, the substantia nigra pars compacta and the subregions of caudate-putamen (CPU) complex, namely, the striatum (Deumens *et al.*, 2002). Although the bilateral model mimics the human condition

more closely, it is not commonly used due to the requirement of intensive nursing of the animals (Cenci *et al.*, 2002). Hence, the unilateral lesion model is more commonly used.

The unilateral lesion model serves as 'within animal control' because the lesioned hemisphere can be compared with the non-lesioned one. Thus, measuring contralateral or ipsilateral rotations is a golden standard for measuring the severity of the lesion (Schwarting & Huston, 1996). The resulting asymmetries in body posture and contralateral sensorimotor deficits have been used to devise simple and objective tests to monitor the effects of symptomatic or restorative treatments (Cenci *et al.*, 2002). However, in the unilateral model the intact side can partly compensate for the affected side by sprouting of dopaminergic projections and this could be the reason why the bilateral model exhibits additional behavioral deficits (Roedter *et al.*, 2001). Nonetheless, the fact that PD affects the human brain bilaterally makes the bilateral 6-OHDA model important for PD research.

6-OHDA injections in both hemispheres result in additional behavioral deficits like weight loss, reduction in locomotor activity and exploratory behavior and a long term deficit in skilled forelimb use measured by reaction time task and fixed-ratio bar pressing task (Roedter *et al.*, 2001). Dopamine dysregulation in the striatum results in hypophagia (reduced food intake) and regulated release of dopamine in the striatum is necessary for normal feeding and other goal directed behaviors (Sotak *et al.*, 2005).This coupled with reduced forelimb dexterity results in sustained weight loss in the bilateral model (Lenard *et al.*, 1991) which is consistent with a report indicating that PD patients have lower weights than their matched controls (Chen *et al.*, 2003). A study by (Westin *et al.*, 2012) shows that bilateral lesions result in gait disturbances and postural instability measured by

several aspects of gait like shorter stride length, decreased swing speed, shorter base of support and increased stance duration as observed in PD patients (Knutsson, 1972).

The 6-OHDA model has also been extensively used to study the time course and extent of dopaminergic loss in the striatum and SNc. Intrastriatal injection of 6-OHDA resulted in early damage of dopaminergic terminals followed by a slowly evolving loss of dopaminergic cell bodies in the SNc, both peaking on the 28th day post lesion (Blandini *et al.*, 2007). This progressive loss of SNc neurons, peaking around 4 weeks has been confirmed by another study involving TH-immunohistochemistry as well as PET imaging (Cicchetti *et al.*, 2002). Another study claims that the cell loss continues until 8 to 16 weeks (Sauer & Oertel, 1994), highlighting the progressive nature of the 6-OHDA model.

1.2.3 Neuroprotection

Due to the progressive dopaminergic cell loss observed in PD patients, neuroprotective therapies which can slow, stop or reverse disease progression are urgently needed. Clinical trials involving antioxidants or dopamine agonists have tried to examine their neuroprotective effects but haven't resulted in clear answers. (Schapira & Olanow, 2004). Neurorestorative therapies like site specific targeted delivery of Glial-Derived Nerve Growth Factor (GDNF) to dopamine (DA) neurons and striatum have shown significant protection or restoration in the MPTP primate model (Kordower, 2000) as well as the 6-OHDA rodent model (Shults *et al.*, 1996). Intrastriatal injections of Brain Derived Neurotrophic factor (BDNF) have also shown to attenuate the effect of 6-OHDA lesions (Shults *et al.*, 1995) and reduce the subsequent rotational behavior (Klein *et al.*, 1999), however a comparative study indicates that GDNF is more effective than BDNF for both

correcting behavioral deficits and protecting nigrostriatal DA neurons (Sun *et al.*, 2005). A recent study involving deep brain stimulation of the Subthalamic nucleus (STN) has shown proof of neuroprotective effect on the SN neurons in a rodent 6-OHDA model (Spieles-Engemann *et al.*, 2010a) while subsequent experiments from the same group observed an increase in BDNF in the nigrostriatal system and primary motor cortex following STN DBS (Spieles-Engemann *et al.*, 2011). However, clinical studies conducted with advanced PD patients to measure disease progression using ^{18}F-fluorodopa PET failed to confirm a neuroprotective effect of clinically effective STN-DBS (Hilker *et al.*, 2005). Thus, although current neuroprotective methods show promise, additional clinical trials are necessary to confirm their efficacy in PD patients (Dawson & Dawson, 2002).

1.2.4 Spinal cord stimulation for PD

With an aim to investigate alternative treatment therapies for PD, (Fuentes *et al.*, 2009) studied the acute effect of dorsal column stimulation on PD symptoms in rodent models. It was observed that DCS treated animals showed higher locomotion than both dopamine depleted mice and 6-OHDA lesioned rats. Increased oscillatory power in 1.5-4 and 10-15 Hz bands and decreased power in 25-55Hz band was observed during the depleted state in mice and the power of oscillations shifted to higher frequencies on the application of stimulation, similar to a state prior to locomotion initiation, suggesting that DCS created a brain state permissible for locomotion. Although, the mechanism of DCS effect on symptoms is not yet clear, the role of corticostriatal desynchronization is highly probable.

It is possible that the synchronous low frequency oscillations in GPi and STN, which are characteristically associated with Parkinsonian symptoms (Bergman *et al.*, 1994; Wichmann & DeLong, 1998; Wichmann & Soares, 2006) keep the motor cortex in a low frequency anti-kinetic state and any intervention that interferes with the oscillations could facilitate the change to a pro-kinetic state (Brown, 2003). A recent study using light activated ion channels shows that stimulation of cortical afferents to the STN and not cell bodies is sufficient for improvement of PD symptoms in the 6-OHDA rodent model suggesting that antidromic activation of cortical pyramidal cells can induce cortical desynchronization (Gradinaru *et al.*, 2009). With the aim to use afferent pathways to achieve cortical desynchronization (Fanselow *et al.*, 2000) showed that trigeminal nerve stimulation could be used to reduce seizure activity in awake rats. Extending this line of thinking further (Fuentes *et al.*, 2009) successfully used dorsal column stimulation to ameliorate PD symptoms. There was strong evidence suggesting that synchronous activation of the dorsal column fibers, leading to the thalamus via the dorsal lemniscal pathways achieved cortico-striatal desynchronization.

Following the publication of these results, premature testing of the technique in two patients with advanced PD did not produce any improvement in motor function (Thevathasan *et al.*, 2010). These preliminary negative results were justified by the significant differences in geometry and spinal level location of the stimulation electrodes utilized (Fuentes *et al.*, 2010). However, after that, a patient diagnosed with PD, previously implanted with a quadripolar spinal cord stimulator at low thoracic level to treat low back pain, experienced dramatic improvement of the PD motor symptoms through high

frequency (130 Hz) DCS (Fenelon *et al.*, 2012). Further, other 15 PD patients treated with DCS for low back and leg pain experienced significant improvement of gait and posture in the long-term (Agari & Date, 2012). Heretofore, all reported results of DCS in Parkinson's animal models and PD patients refer to acute use of this stimulation method and an understanding of the long term implications of DCS on Parkinsonian symptoms needs to be fulfilled.

1.3 Artificial somatosensation

Brain machine interfaces have enabled the use of cortical neurons for controlling artificial actuators and robotic devices, however, the movements generated are often unstable and slow. This could be due to the lack of tactile or proprioceptive feedback, from the prosthetic limb, which can provide information about, the objects in contact or spatial location of the limb. To this effect numerous approaches have been made to generate artificial sensory sensations using intracortical microstimulation (ICMS) of the somatosensory cortex (S1). A study by (Romo *et al.*, 1998; Romo *et al.*, 2000) showed that, rhesus monkeys can discriminate between two sensations similar to the perception of flutter, generated by ICMS of area 3b of S1 using different stimulation frequencies. Subsequently, an artificial sense of proprioception created by ICMS of area 3a of S1 was successfully used by monkeys to discriminate between trains of different frequencies (London *et al.*, 2008). Similarly, it has also been shown that owl monkeys learnt to discriminate different spatio-temporal patterns of stimulation delivered to the primary somatosensory cortex (Fitzsimmons *et al.*, 2007). A study involving DBS patients showed

that microstimulation of thalamic nuclei with varying stimulation patterns produced somatotopically organized percepts in the patient's body suggesting that the thalamus could be a potential site for sensory prosthetic feedback (Heming *et al.*, 2010). Doherty and colleagues have demonstrated a brain machine brain interface, where somatosensory feedback was provided in real time, using ICMS of S1, while monkeys simultaneously continued using their cortical signals, for moving an avatar arm over multiple virtual textures (O'Doherty *et al.*, 2011). Recently, optogenetic stimulation of S1 has also shown promise for generating artificial tactile sensation in non-human primates, similar to those obtained by electrical stimulation (May *et al.*, 2014). Although, various locations along the afferent sensory pathway have been explored for producing artificial sensations, right from the periphery using targeted reinnervation of nerves (Marasco *et al.*, 2009) to the somatosensory cortex (Weber *et al.*, 2012), the role of epidural spinal cord stimulation, for producing discriminable percepts for sensory feedback, has never been explored. Previous animal studies involving intraspinal microstimulation aimed at recruiting motor neurons have achieved the recruitment of sensory afferents (Gaunt *et al.*, 2006), however, it remains undetermined, if spinal cord can be a site for producing artificial sensations of the type elicited by ICMS of S1 and thalamus.

1.4 Brain to Brain communication

Recent advancements in Brain Machine Interface research have led to the emergence of a new paradigm of communication between two brains called Brain-to-Brain-Interfaces (BTBI) where, information decoded from one brain is encoded into

another brain, using a direct interface. The first demonstration of a BTBI was performed by (Pais-Vieira *et al.*, 2013a) where, sensorimotor information from an encoder rat was sent to the cortex of decoder rat, over the internet, resulting in a dyad, which showed dynamic behavior, depending on the relative performances of both animals. Subsequently, (Grau *et al.*, 2014) created the first conscious brain to brain interface in humans where, pseudorandom binary streams encoding words were sampled from the encoder, using voluntary motor imagery controlled electroencephalography (EEG) and transmitted to the decoder's brain as conscious perceptions of phosphenes i.e. light flashes, using transcranial magnetic stimulation (TMS). Similarly another report from (Rao *et al.*, 2014) demonstrated the real-time transfer of motor commands from encoder to decoder using EEG for decoding and TMS for actuation of the decoder's arm. Recently, it has been shown that multiple brains of rats can be connected to create an organic computing device or 'brainet' that can perform a number of computations such as discrete classification, image processing, storage and retrieval of tactile information (Pais-Vieira *et al.*, 2015) or that multiple non-human primates can modulate their neuronal activities together to create a dynamic 'brainet' that can perform an arm movement task (Ramakrishnan *et al.*, 2015).

Although, BTBIs raise several ethical implications like neural privacy, cognitive enhancement, coercion and nature of personhood (Trimper *et al.*, 2014), it won't take too long before BTBIs enabling the transfer of emotions and other cognitive information emerge or BTBIs get appropriated for the treatment of neurological disorders.

1.5 Organization

In chapter 2, I investigated long term effects of dorsal column stimulation (DCS) on the symptoms of Parkinson's Disease (PD) in a 6-hydroxydopamine rat model. I studied the use of DCS as a technique for therapy from a neurological disorder (in this case PD) based on the hypothesis that DCS causes long-term changes in supraspinal structures. The experiments were conceived with substantial advice from Romulo Fuentes. The experiments and spinal cord implants were performed by myself. I was assisted in the lesion procedures by Hao Zhang and Click Wang. Immunohistochemistry was done by Thais Vinholo and Marco Freire. The results in this chapter have been published (Yadav *et al.*, 2014).

In chapter 3, I used DCS as a technique to generate artificial tactile sensations and train rats to discriminate multiple DCS induced tactile percepts, while in chapter 4, I developed the first of its kind real-time brainet for cortico-spinal communication. Both ideas were based on the hypothesis that DCS can be used as an effective channel to communicate with the brain. Spinal cord electrodes and neuronal recording arrays were implanted by myself. I was assisted on the experiments by Daniel Li. I was the main contributor to the analyses. The results are currently being prepared for submission.

2. Chronic Spinal Cord Electrical Stimulation Protects Against 6-hydroxydopamine Lesions

2.1 Abstract

Although L-dopa continues to be the gold standard for treating motor symptoms of Parkinson's disease (PD), it presents long-term complications. Deep brain stimulation is effective, but only a small percentage of idiopathic PD patients are eligible. Based on results in animal models and a handful of patients, dorsal column stimulation (DCS) has been proposed as a potential therapy for PD. To date, the long-term effects of DCS in animal models have not been quantified. Here, we report that DCS applied twice a week in rats treated with bilateral 6-OHDA striatal infusions led to a significant improvement in symptoms. DCS-treated rats exhibited a higher density of dopaminergic innervation in the striatum and higher neuronal cell count in the substantia nigra pars compacta compared to a control group. These results suggest that DCS has a chronic therapeutic and neuroprotective effect, increasing its potential as a new clinical option for treating PD patients.

2.2 Introduction

Parkinson’s disease (PD) is a debilitating neurodegenerative disorder caused by progressive loss of the dopaminergic neurons of the nigrostriatal pathway (Carlsson, 1972). A variety of pharmacological approaches, of which Levodopa (L-dopa) administration is

the most effective, have been used to alleviate PD motor symptoms by supplementing the dopamine (DA) deficiency observed in the striatum (Nagatsua & Sawadab, 2009). Despite its initial efficacy, long-term administration of L-dopa results in fluctuations in the clinical response and in L-dopa-induced dyskinesia (LID), a condition which is difficult to treat (Nagatsua & Sawadab, 2009).

The therapeutic approach involving electrical stimulation of subcortical nuclei, known as deep brain stimulation (DBS), is also very effective in alleviating the motor symptoms of PD (Benabid, 2003). The best candidates for this treatment are idiopathic PD patients with motor fluctuations and L-dopa-induced dyskinesia (Benabid, 2003). Depending on the selection criteria, 1.6 to 4.5% of PD patients are eligible for subthalamic nucleus DBS (Morgante *et al.*, 2007), making DBS available only to a small percentage of the overall population of PD patients.

Based on previous results obtained in three different rodent models of PD(Fuentes *et al.*, 2009), we have proposed that a new neuromodulation procedure that does not invade the brain tissue, known as dorsal column stimulation (DCS), has the potential to emerge as an additional therapeutic option for PD patients. In our hands, the most effective DCS effects in rodent PD models were obtained when continuous high frequency electrical stimulation was delivered to the large superficial fibers, running through the dorsal columns of the spinal cord, by a transversally oriented stimulating electrode, implanted at the high thoracic segments of the cord.

Following the publication of our animal study, a hasty testing of DCS in two patients with advanced PD was carried out. This study did not produce any improvement

in motor function (Thevathasan *et al.*, 2010). However, these initial negative results were easily explained by the significant methodological differences between the stimulation protocols employed in the animal and clinical studies. These included: the localization of the electrodes (high cervical in the human study vs. high thoracic in the rodent study), and the orientation of the electrode poles relative to the spinal cord (longitudinal in the clinical study vs. transversal in the animal experiments). These differences caused the effective surface of contact between the electrodes and the spinal cord to be around seven times larger in the rodent protocol when compared to the human study. Such a marked difference could account for the activation of substantially more ascending dorsal column fibers in the rodents, explaining why such a potent therapeutic effect was observed in the animal study and absent in the clinical one (Nicolelis *et al.*, 2010).

Soon after, however, support for our hypothesis that DCS can be effective as a PD therapy was subsequently obtained with the publication of four other clinical reports. These studies clearly indicated that DCS, originally intended for treating chronic pain, led to significant alleviation of motor symptoms in a total of 18 PD patients. For example, a PD patient, who had been previously implanted with a quadripolar spinal cord stimulator at low thoracic level to treat low back pain, experienced significant improvement of his motor symptoms during high frequency (130 Hz) DCS (Fenelon *et al.*, 2012). Furthermore, DCS also produced significant improvement of gait, posture, stability, and bradykinesia in 15 PD patients who received a spinal cord implant designed to treat low back and leg pain (Agari & Date, 2012). Next, a patient with advanced PD and other sensory symptoms also experienced improvement in gait and posture with quadripolar DCS applied at thoracic

level (Landi *et al.*, 2012). Lastly, a female patient with PD and chronic neuropathic pain, experienced increasing improvement of motor PD symptoms over a two year period after initiating the DCS treatment. This improvement included alleviation of tremor and rigidity, and an improvement in gait and posture (Hassan *et al.*, 2013a).

In our view, the pro-kinetic effect of DCS described in animal models and in several PD patients could be explained by the activation of somatosensory fibers, running through the dorsal column of the spinal cord, which led subsequently to the modulation of the ongoing activity of somatosensory and motor supraspinal structures (Stancak *et al.*, 2008; Fuentes *et al.*, 2009; Aguilar *et al.*, 2011). Accordingly, in our original study, we observed that the motor effect of DCS is almost instantaneous and lasts as long as the electrical stimulation is maintained (see the supplementary video from previous studies (Fuentes *et al.*, 2009; Fenelon *et al.*, 2012)).

Up to now, however, the results reported with spinal cord stimulation in animal models of PD have been limited to its acute effect. Nonetheless, DCS is also known to cause changes in gene expression at supraspinal structures, which in turn may lead to long-term sustained effects (Dejongste *et al.*, 1998; Maeda *et al.*, 2009). In the present study, therefore, we explored, for the first time, the potential effects of chronic delivery of DCS in rats with bilateral intrastriatal 6-hydroxydopamine (6-OHDA) lesions. While the lesioned rats exhibited sustained weight loss, postural and gait abnormalities, paralleled by destruction of dopaminergic striatal projections, a group of DCS-treated animals showed a dramatic and consistent reversal of these signs, including significant gain of body weight gain, marked improvement in motor functions, and less dopaminergic neuronal loss

throughout the nigrostriatal system. These results are compatible with a neuroprotective effect of DCS against chemically induced dopaminergic lesions, and suggest that DCS could have long-term benefits as a potential new therapy for PD.

2.3 Methods

2.3.1 Animals

A total of 41 male Long-Evans rats (body weight ranging from 310 to 450 g) were housed individually with ad-libitum food and water in a temperature controlled room on a 12h light/12h dark cycle. Animal procedures were performed according to prior approved protocols by Duke University Institutional Animal Care and Use Committee and in accordance with the National Institute of Health Guide for the Care and Use of Laboratory Animals (NIH Publications No. 80-23). Rats were divided into 3 groups (sham control, 6-OHDA lesion and 6-OHDA lesion + DCS).

2.3.2 Stimulation electrode implant procedures

Rats in the 6-OHDA + DCS group underwent two separate surgical procedures. First, they were implanted with spinal stimulation electrodes under anesthesia induced with 5% halothane, ketamine (100mg/kg), xylazine (10mg/kg) and atropine (0.05ml). Postoperative weight was monitored daily. The stimulation electrodes used for DCS consisted of two parallel rectangular plates of platinum (3x0.75x0.025 mm) separated by 1mm (Fig 2.1 A). Each plate was micro-soldered to 7-strand coated steel wire 30 cm long, arranged longitudinal to the plates. Surgical thread (5cm) was placed between the platinum plates and the entire assembly was covered with surgical silicone, keeping in mind to leave

the surface opposite the wire connection exposed. The electrodes were implanted in the dorsal spinal cord, in the epidural space below thoracic vertebra T2 (Fig 2.1 B). The surgical thread was tied to T2 to provide stability for long term stimulation and prevent electrode migration. Once the electrode was in position, the connecting wires were projected between T2 and T3 and were curved to form a loop to prevent pushing or pulling of the electrodes. The wires were then subcutaneously directed towards the skull where they were attached to a connector fixed to the skull. External programmable stimulator (Master-8) was connected via a stimulus isolator unit (ISO-FLEX) to the connector for the delivery of DCS.

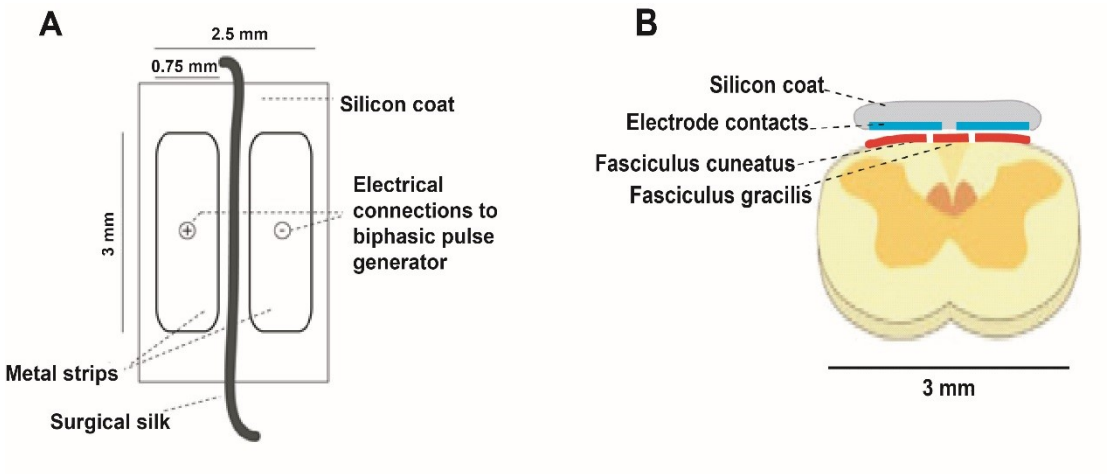

Figure 2.1 DCS electrode design and implantation. A) Schematic dorsal view of DCS electrode. B) Transverse plane of a rodent spinal cord with DCS electrode

2.3.3 6-OHDA lesion

One week later, after recovery of initial weight, rats were anesthetized for a second surgery, with 5% halothane, followed by intramuscular injections of ketamine (100mg/kg), xylazine (10mg/kg) and atropine (0.05ml). A total of 52.5ug 6-OHDA hydrobromide

(Sigma Company, USA - 3.5 mg/ml in 0.05% ascorbate saline) was injected bilaterally into the striatum, at 3 locations on each side, using a needle, driven by a syringe pump (Sage, Model 361, Firstenberg Machinery Co Inc., USA) via 10uL Hamilton syringe, at 1uL/min. The needle was left in situ for 5 minutes and withdrawn slowly, to prevent backtracking of the drug. Anteroposterior, mediolateral and dorsoventral coordinates for the injections were: +1.0, +/-3.0, -5.0; -0.1, +/-3.7, -5.0 and -1.2, +/-4.5, -5.0 (Winkler *et al.*, 2002) from bregma. Destruction of noradrenergic fibers and terminals was prevented by 1,3-Dimethyl-2-imidazolidinone (DMI, Sigma Company, 25 mg/kg), administered IP, 30 minutes prior to 6-OHDA treatment (Hrdina & Dubas, 1981).

Rats belonging to the 6-OHDA lesion and sham control groups underwent only the surgical procedure required to perform the lesion; animals in the 6-OHDA lesion group received bilateral injections of 6-OHDA, while rats in the sham control group received only vehicle solution (0.05% ascorbate saline). Time course of the entire experiment is shown in Fig. 2.2. The lesion procedures were performed by the same individuals throughout the experiment and all groups were run in parallel. Extreme care was taken to consistently maintain the timing of the various methods and conditions during the lesion procedure.

2.3.4 Weight and Motor Behavioral Assessment

In the post-lesion period, rats had access to water soaked food pellets and fruit loop cereals and their body weight was recorded daily. 15 rats that did not display severe motor symptoms and lost less than 20% of initial weight at day 7 post-lesion were discarded from the experiment. Rats with severe weight loss (>20% body weight) were retained in their original groups and subjected to the entire experiment (N=18, 10 in 6-OHDA lesion + DCS

group, and 8 in 6-OHDA lesion group). These were labeled as “strongly lesioned rats”. Rats that lost more than 25% of initial weight were additionally hand-fed with peanut butter daily, until their weight reached 75%.

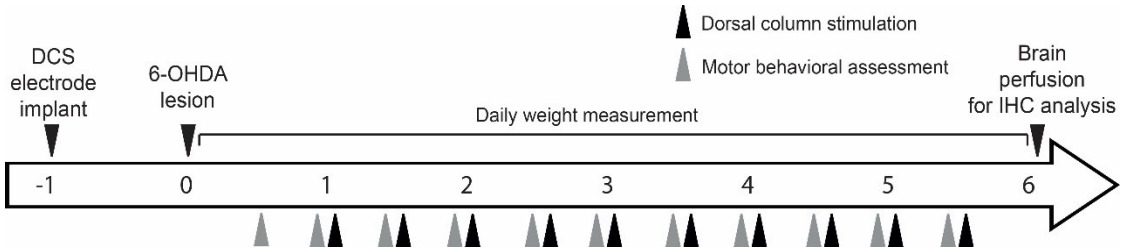

Figure 2.2 Time course of the experiment. Numbers indicate experimental weeks from onset at time 0 (6-OHDA lesion). Rats in 6-OHDA+DCS group sustained epidural DCS electrode implantation (week -1) 1 week before the 6-OHDA lesion (week 0). Rats in 6-OHDA and sham control groups underwent only bilateral lesion procedure; 6-OHDA group (total 52.5 µg 6-OHDA), sham control group (only vehicle solution). Timing of motor assessment and 30 minute DCS sessions is illustrated by grey and black upward arrows respectively. Six weeks post lesion (week 6), brains were collected and processed for immunohistochemistry (IHC).

A few days after lesioning, strongly lesioned rats exhibited several motor impairments, including postural and gait instability, and reduced forelimb dexterity (Deumens *et al.*, 2002). These symptoms manifested into an inability to grasp or chew food, which was clearly observed while the rats tried to eat. Motor behavior was assessed twice a week, on days 4, 7, 11, 14, 18, 21, 25, 28, 32, 35, and 39 post lesion. Rats were placed in an elliptical open field (85cm x 70cm axes, 60cm tall) for 30 min and motor behavior was recorded from a bottom view camera.

The posture and position of the rats in the open-field was extracted from digitized video recordings with custom designed algorithms implemented in Matlab (MathWorks, USA). Image processing of single frames from the video was used to extract the rat shape.

An ellipsoid was fitted to the rat shape, and the length of the major axis of the ellipse (expressed in pixels) was used as a measure of posture. Digital videos of the ellipse superimposed on rat shape were saved and later used to confirm the accuracy of the algorithm. We observed that rats with crouched posture had shorter major axis length, while normal rats had longer lengths. For posture analysis only those frames during which the rats were mobile were used. Instantaneous speed and instantaneous acceleration vectors were calculated from the distance between the X,Y location of the rat every 1/30 seconds in the open field. Lesioned rats showed jerky movement that lacked smoothness and fluidity. To quantify this abnormal behavior, we calculated the derivative of the instantaneous speed, thus obtaining a measurement of instantaneous acceleration. A spectrogram with a window of 4 seconds, sliding every 0.033 seconds was constructed with the 'mtspecgramc' function (Chronux toolbox) from the acceleration signal. The power spectra between 0.5-4.75 Hz of the time bins where locomotion was greater than 5 cm/s were averaged. For measuring stride length of rats, videos from top view camera were used. The front most part of the camera view was selected for better visualization of hind legs. A locomotion bout with at least 3 strides in the selected part of the open field was randomly selected from entire session and stride length was measured using ‘implay’ function in Matlab and averaged for the 3 strides. Stride was defined as the pixel distance between hind leg (right/left) take off point and subsequent landing point of same leg.

2.3.5 Chronic Electrical Stimulation of the Dorsal Column of the Spinal Cord

After the 30 min behavioral session, rats of the 6-OHDA + DCS group were allowed to rest in their home cage for 30 min. Following this period, they were reintroduced

in the open field and continuous DCS was applied for 30 min. Before each stimulation session, stimulation current intensities were determined for each rat such that they caused a paresthesia effect as described in a previous study (Fuentes *et al.*, 2009). DCS consisted of biphasic square pulses of 1ms duration, delivered at 333 Hz at a current intensity ~1.2 times the sensory threshold (mean ± sd, intensity at 333 Hz was 167 ± 52 μA). These intensities ensured that DCS did not cause an arousal effect (Fuentes *et al.*, 2009).

2.3.6 Tyrosine Hydroxylase staining and quantification

Forty-two days after lesion, animals were perfused with 4% paraformaldehyde and the brains were kept in 30% sucrose until sectioning. During tissue sectioning, 30μm free-floating sections were obtained from the striatum (AP: 2 to -1) and substantia nigra (SN) (AP: -4.2 to -6.6), defined according to the rat brain Atlas (Paxinos & Watson, 1997). Tyrosine hydroxylase (TH) immunohistochemistry was used to study the extent and position of striatal lesions and quantify the depletion of dopaminergic neurons in the nigrostriatal pathway as described elsewhere (Tischler, 1995).

For quantification of TH-staining, the tissue samples were mounted and pictures were taken using a microscope with the same camera configuration and light intensity for each slice. TH-reactivity in both striatum and substantia nigra pars compacta (SNc) in all groups (sham control, 6-OHDA lesion and 6-OHDA lesion + DCS) was assessed by computer densitometry using digital images captured with the camera attached to the microscope. Average densitometric values were obtained by using the ImageJ software (http://rsb.info.nih.gov/ij/) from 2 images where both structures could be

unequivocally defined (see Figure 3). The measurements were obtained inside a 0.04 mm² square window positioned across the structures of interest. In order to evaluate the general TH-reactivity throughout the striatum and SNc we obtained three samples per structure. To minimize the effects of within-group variability, we adopted a normalized scale based on the non-reactive cortical white matter (averaged over measurements of 3 different sites using the same window). For every animal a contrast index was calculated using the following equation (Freire *et al.*, 2007),

$$C = (S-W)/(S+W), \quad (2.1)$$

where, the average optical density (OD) for the striatum or SNc is denoted by 'S' and for the cortical white matter is denoted by 'W'.

Using a high-magnification microscope (NIS-element, Nikon, Japan) equipped with a software package, a total of 6 SNc slices between AP: 5.8 - 6.33 mm of bregma were used to bilaterally count immunoreactive neurons and an average cell count was calculated for every animal. To obtain an unbiased estimate of cell numbers, we applied the Abercrombie's correction factor (Abercrombie, 1946), which compensates for the over counting of sectioned profiles, using the equation

$$P = A*[(M/(M+L)], \quad (2.2)$$

where P is the corrected value, A is the raw density measure, M is the section's thickness (in micrometers) and L is the average diameter of cell bodies (n=40 by group) along the axis perpendicular to the plane of section. The mean value of TH-IR nigral neurons for each animal was expressed as a percentage of cell loss, compared to the mean cell count for sham control rats.

2.3.7 Statistical Analysis

All results are expressed as mean ± sem. Statistical analysis was performed using a computer program (Graphpad Prism 5.0, Graphpad Software, USA). Weight and motor behavior data was subjected to two-way analysis of variance (ANOVA) with repeated measures, followed by post-hoc multiple comparison tests. Whenever distributions failed the normality test, non-parametric tests such as Mann-Whitney (t-test) were used. Spearman's Rank Correlation test was used to study the correlation between different parameters.

2.4 Results

2.4.1 Chronic DCS prevents severe body weight loss in 6-OHDA lesioned rats.

Rats received a bilateral 6-OHDA striatal or a sham lesion, and their weight and motor symptoms were evaluated for a period of 6 weeks (See Fig. 2.2 for time course of the experiment). While the sham lesion surgery, conducted on a group of control rats, caused minor weight loss that was recovered almost immediately, bilateral intrastriatal 6-OHDA lesions resulted in sustained weight loss (Fig. 2.3a). Twice a week DCS treatment (30 minutes per session) caused a dramatic recovery of body weight in 6-OHDA lesioned rats. Indeed, DCS treated animals not only recovered significantly faster than non-treated 6-OHDA rats; their weights were significantly higher from the 11th day post lesion to the end of the experiment (Day 11, $p < 0.05$; days 12-14, $p < 0.01$; days 15-42, $p < 0.001$, Bonferroni multiple comparisons, DCS treated compared to non-treated Fig 2.3a).

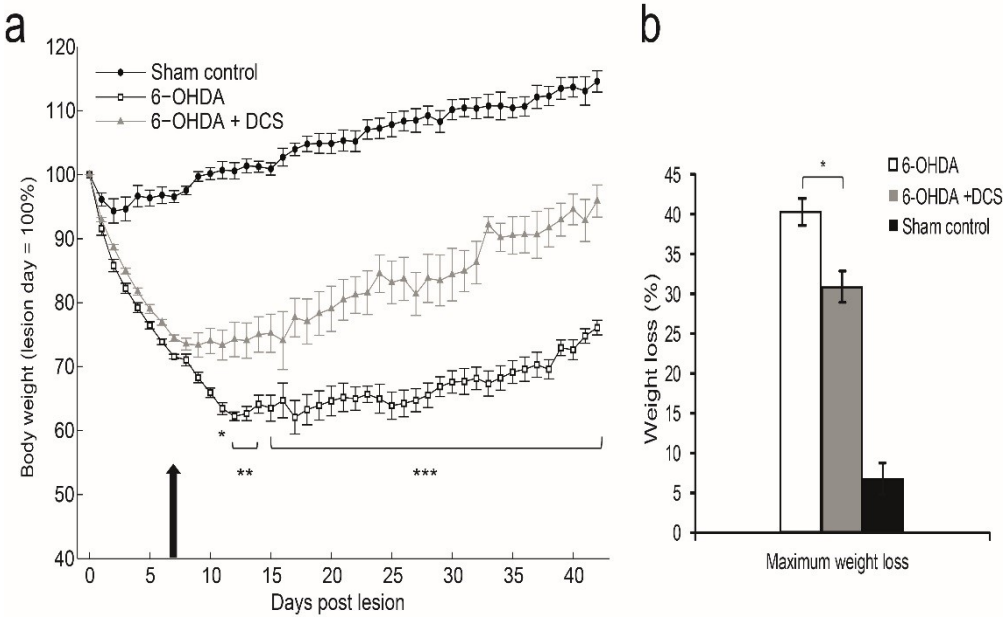

Figure 2.3: Changes in body weight after bilateral intrastriatal 6-OHDA lesion with or without DCS treatment. a) Lesioned, non-treated rats (n=8) suffered sustained weight loss with little-to-none recovery. Lesioned rats with DCS treatment (n=7, 30 min, 333Hz continuous DCS during 30min twice a week, starting 7th day, black arrow) recovered body weight significantly faster than non-treated rats ($p<0.0001$, two-way repeated measure ANOVA). *:$p<0.05$(day 11), **:$p<0.01$(days 12-14), ***:$p<0.001$(days 15-42), Bonferroni multiple comparisons. b) Maximum weight loss is significantly larger for non-treated rats compared to DCS treated rats. *:$p<0.05$, Mann-Whitney test.

Even though the body weight of both 6-OHDA and 6-OHDA+DCS rats was significantly lower than that of the sham control animals throughout the experiment (ANOVA, two factor experiment with repeated measures, groups x days interaction: $p < 0.0001$), by the 6th week, the weight of DCS treated rats approached that of the control rats much more than non-treated animals.

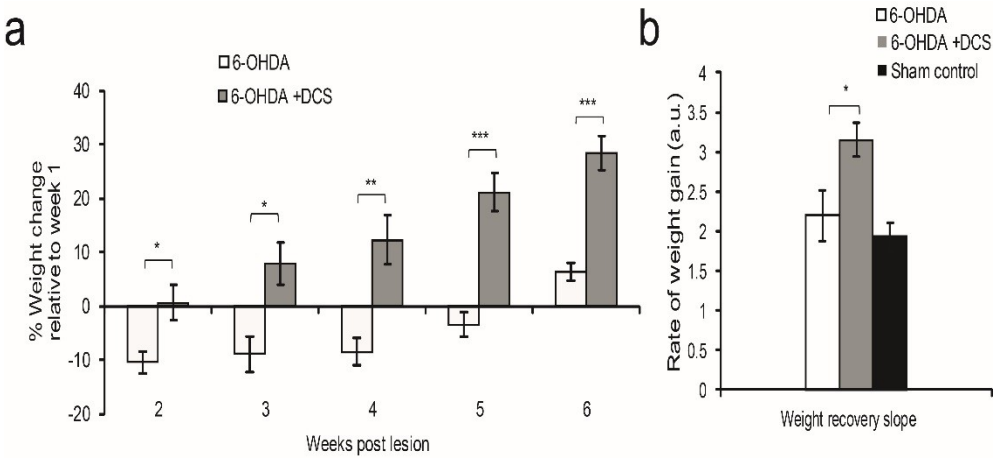

Figure 2.4: DCS treatment results in faster weight recovery. a) DCS treatment reverses the trend of weight loss almost immediately, while non-treated rats continue to lose weight till week 5 as shown by weight change relative to week 1, which is significantly higher for treated rats as compared to non-treated. *:p<0.05, **:p<0.01, ***:p<0.001, Mann-Whitney test. b) Rate of weight gain is significantly higher in treated rats compared to non-treated. *:p<0.05, Mann-Whitney test, a.u. (arbitrary unit). All error bars are s.e.m.

In addition to faster weight recovery, DCS also prevented severe weight loss in lesioned rats during the early period after lesioning. 6-OHDA+DCS treated rats had a maximum weight loss ([30.94 ± 1.96]% ~9 days post lesion) that was significantly lower than non-treated 6-OHDA rats ([40.35 ± 1.68]% ~15 days post lesion, $p<0.05$, Mann-Whitney test, Fig 2.3b). Weight recovery of 6-OHDA+DCS rats began in week 2 and continued to improve until week 6, while non-treated 6-OHDA rats started weight recovery only in the 6th week, implying that chronic DCS almost immediately reversed the trend of weight loss. Fig. 2.4a shows that after initiation of DCS treatment, weight change (normalized to week 1) was significantly higher at every time point for treated rats as compared to non-treated subjects: week 2 (0.68 ± 3.37, -10.38 ± 2.08, $p<0.05$), week 3

(7.92 ± 3.95, -8.87 ± 3.26, $p<0.05$), week 4 (12.26 ± 4.52, -8.46 ± 2.57, $p<0.01$), week 5 (21.19 ± 3.52, -3.42 ± 2.3, $p<0.001$) and week 6 (28.45 ± 3.23, 6.32 ± 1.66, $p<0.001$; all measurements obtained with Mann-Whitney test).

The slope of body weight recovery, calculated from a line connecting the minimum weight value with the final day value, was also higher for DCS treated rats than non-treated rats, (3.15 ± 0.21 vs. 2.2 ± 0.33, $p<0.05$, Mann-Whitney test, Fig. 2.4b) confirming that chronic DCS not only prevented sustained weight loss by initiating weight recovery earlier, but it also accelerated the process of weight recovery in the 6-OHDA lesioned rats.

2.4.2 Long term DCS restores motor function in PD rats.

Bilateral intrastriatal lesioning with 6-OHDA resulted in a significant loss of motor function. Lesioned rats developed a characteristic crouched posture, which we quantified from video images by measuring the length of the major axis of an ellipse fitting the animal's body. The crouched posture of the 6-OHDA rats resulted in an axis length shorter than in control rats. Quantitative analysis revealed that there was a significant interaction between groups and weeks (ANOVA, two factor experiment with repeated measures, groups x weeks: $p<0.05$). Thus, starting at week 1.5, a gradual reversal of posture abnormalities was observed in the chronic DCS treated rats. Fig. 2.5 shows that axis length was significantly higher for 6-OHDA+DCS rats (n=6) for week 3.5 (63.59 ± 0.74 versus 56.54 ± 2.10, $p<0.05$) and 4.5 (64 ± 1.79 versus 56.37 ± 1.79, $p<0.05$) as compared to non-treated rats, n=8 (Bonferroni multiple comparisons). Overall, 30 min continuous DCS twice a week was sufficient to restore normal posture in 6-OHDA lesioned rats.

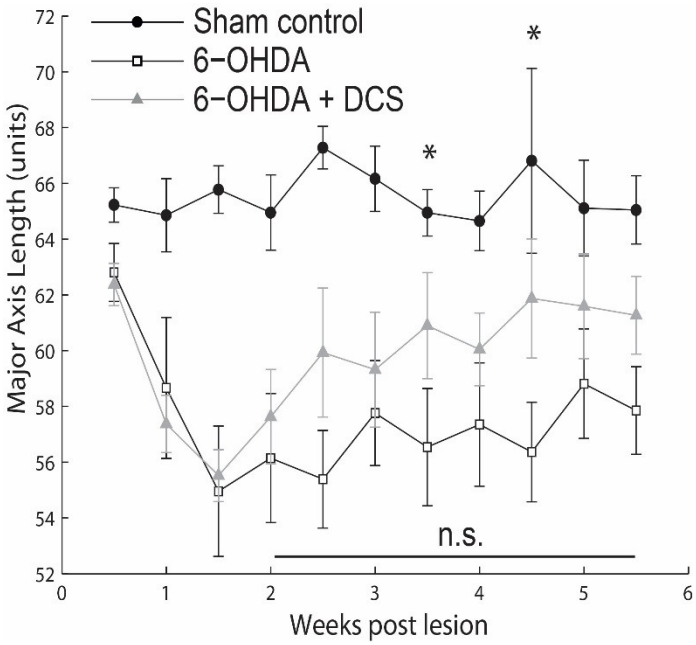

Figure 2.5: Changes in rat posture with or without DCS treatment. Lesioned rats develop crouched posture resulting in shorter major axis length. DCS treatment restores posture significantly faster than non-treated rats [groups x weeks interaction: $p<0.05$, two-way repeated measure ANOVA, *:$p<0.05$ at week 3.5 and 4.5 between DCS treated (n=6) and non-treated rats (n=8), n.s.: DCS treated rats were not significantly different from controls (n=4) from week 2, Bonferroni multiple comparisons].

Lesioned rats in this study showed no significant differences in the distance traveled during a 30 min open field session between the control and the DCS treated animals (Fig. 2.6a). Nonetheless, control rats showed a progressive decrease in traveled distance over the weeks, while 6-OHDA rats, both treated and non-treated, showed an irregular pattern (ANOVA, two factor experiment with repeated measures, groups x weeks interaction: $p <$

0.0001, but no differences were seen on post-hoc analysis). In the same way, the average speed displayed in the open field did not show significant differences between the groups (Fig. 2.6b, ANOVA, two factor experiment with repeated measures, groups x week interaction: $p < 0.01$, no differences on post-hoc analysis).

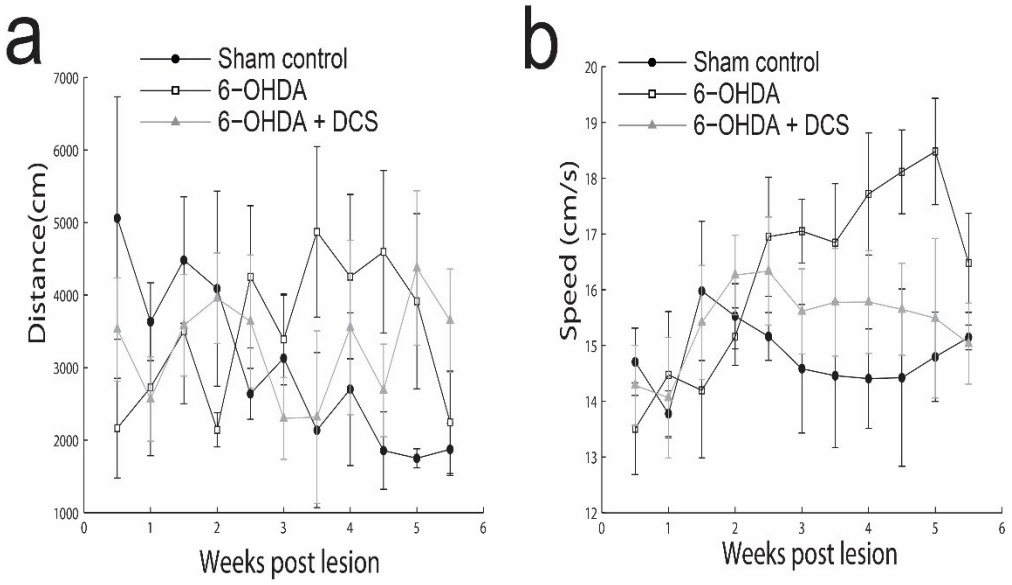

Figure 2.6: Effect of DCS on distance traveled and speed. a) Distance travelled and b) average speed during a 30 min open field session was not significantly different between the groups (groups x weeks interaction: $p < 0.0001$ for distance, groups x weeks interaction: $p < 0.01$ for speed, but no differences on post-hoc analysis for both).

We observed that the 6-OHDA rats lacked fluidity and smoothness during locomotion. This is evident in the example shown in (Fig 2.7) in the top row, depicting the instantaneous speed (obtained by calculating the distance between the positions of the rat

every 0.033 seconds) of a control (left), a 6-OHDA (middle) and a 6-OHDA+DCS (right) rat during a locomotion bout. To quantify the lack of smoothness of the 6-OHDA rat locomotion, we calculated the derivative of the instantaneous speed, thus obtaining the instantaneous acceleration (middle row).

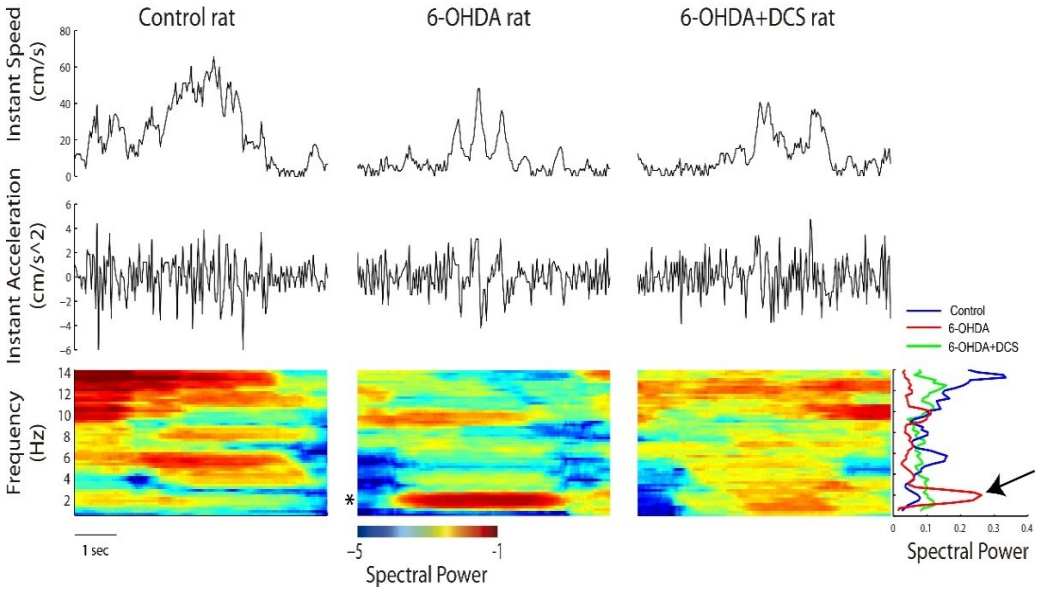

Figure 2.7: 6-OHDA lesioned rat resulted in jerky non-smooth locomotion. (Top row) Instantaneous speed, (Middle row) Instantaneous acceleration i.e. derivative of instantaneous speed, (Bottom row) Spectrogram of Instantaneous acceleration showing strong power at 2Hz for 6-OHDA rat (middle) as compared to control or 6-OHDA+DCS rat (left and right). (Bottom row, 4th panel) Average power of spectrogram showing 2Hz peak (arrow)

A spectrogram with a window of 4 seconds, sliding every 0.033 seconds was constructed with the 'mtspecgramc' function (Chronux toolbox, MATLAB) from the acceleration signal. While locomotion bouts of 6-OHDA rats showed strong power around 2 Hz (third row, middle panel, asterisk), the frequency of the observed jerky gait, this was

not observed in the control rats neither in the DCS treated rats (third row, right and left panel). The average power of each example spectrogram is shown in the fourth panel of the bottom row, with the 6-OHDA power spectra (red line) showing a strong peak at 2 Hz (arrow), absent in both control and 6-OHDA+DCS power spectra (blue and green, respectively).

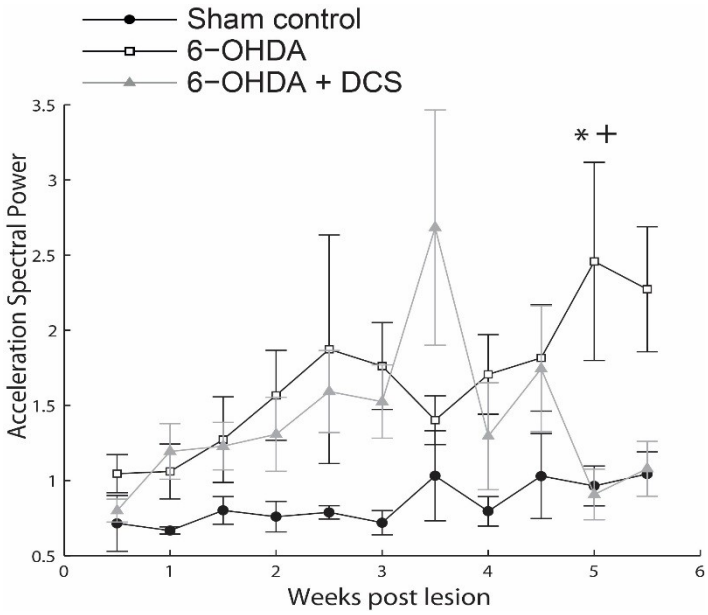

Figure 2.8: Effect of DCS on jerky non-smooth locomotion. Spectral power of the acceleration vector in frequency range 0.5-4.75Hz (indicating jerky non-smooth locomotion) was significantly higher in lesioned rats than DCS treated and controls towards the end [p<0.05, two-way repeated measure ANOVA, *:p<0.05 (6-OHDA+DCS compared to 6-OHDA), +:p<0.05 (6-OHDA compared to controls), Bonferroni multiple comparisons].

The symptom of rigid gait and non-smooth locomotion in untreated rats was quantified by calculating the spectral power at the frequency range of 0.5-4.75 Hz of the

instant acceleration vector of the rat displacement: high power values represent a jerky, non-smooth gait (Figure 2.8), compatible with rigidity and crouched posture. DCS treated rats, on the other hand, showed a much lower spectral power in the same frequency (0.5-4.75Hz) of instant acceleration vector. This allowed DCS-treated rats to exhibit a smoother gait, suggesting that DCS had an effect in improving animal locomotion. Overall, there was a significant interaction between groups and weeks in the spectral power of the acceleration vector (Fig 2.8, ANOVA, two factor experiment with repeated measures, groups x weeks: $p < 0.05$). At week 5, lesioned rats (2.46 ± 0.66) had higher spectral power than both DCS treated (0.91 ± 0.17) and control animals (0.96 ± 0.13), $p<0.05$, Bonferroni multiple comparisons. Again, this finding suggests that the DCS treatment had a significant effect in improving motor behavior in lesioned animals.

Further, the length of the stride was measured at week 4 for animals in the three groups. Untreated lesioned rats (58.74 ± 2.59) had shorter strides as compared to both DCS treated (69.12 ± 2.77) and control animals (79.05 ± 4.02), however the stride length of treated rats was not significantly different from that of controls (One-way ANOVA, $p<0.01$, Tukey's Multiple Comparison test, Fig 2.9)

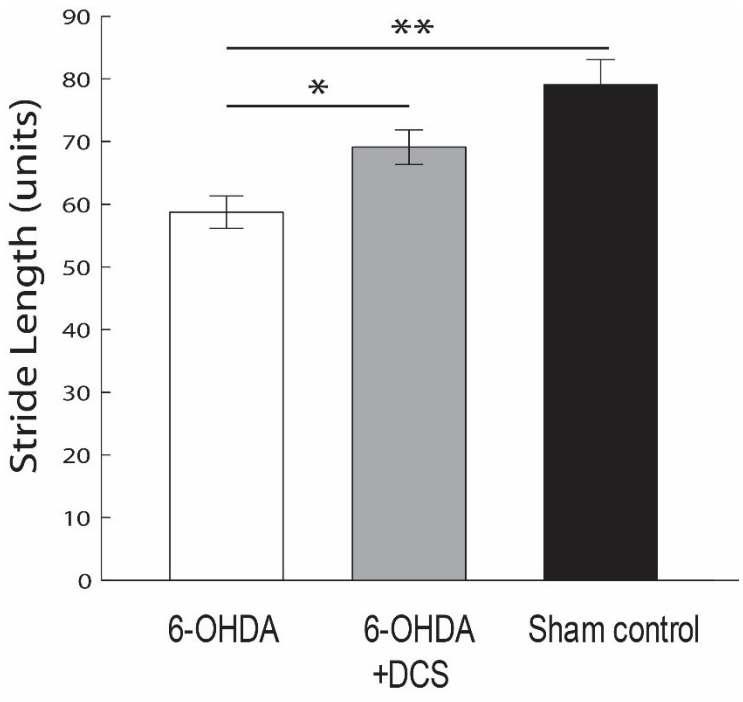

Figure 2.9: Effect of DCS on stride length. Stride length measured at week 4 was significantly higher for DCS treated rats as compared to non-treated ($p<0.01$, one-way ANOVA, *:$p<0.05$, **:$p<0.01$-Tukey's multiple comparison test). All error bars are s.e.m.

2.4.3 Long-term DCS protects nigrostriatal dopaminergic system

6-OHDA lesions resulted in severe damage to nigrostriatal dopaminergic striatal projections as compared to sham controls, as evidenced by the loss of TH immunoreactivity in these areas (Fig. 2.10a, bottom and middle panels). Quantification of the striatal TH immunoreactivity by a contrast index (CI) showed significant differences when the three groups were compared (one-way ANOVA, $p<0.05$, Fig. 2.10c, top panel). 6-OHDA lesioning caused a 67% decrease of striatal TH levels when compared to the sham

control group (6-OHDA CI 0.114 ± 0.022, sham lesion 0.34 ± 0.024; Bonferroni's Multiple Comparison, $p<0.05$). However, DCS treatment of the 6-OHDA lesioned rats resulted in a 35% decrease of striatal TH levels. The difference between the TH levels of the 6-OHDA and 6-OHDA+DCS groups (around 32% of the TH control levels) was significant (6-OHDA+DCS CI 0.222 ± 0.018, 6-OHDA CI 0.114 ± 0.022, Bonferroni's Multiple Comparison, $p<0.05$).

Similarly, 6-OHDA lesioning resulted in a severe loss of TH immunoreactivity, measured by the contrast index in the subtantia nigra pars compacta (SNc), as shown in the example in Fig. 2.10b. Six weeks after lesioning, 6-OHDA rats showed a significant decrease in TH CI (0.106 ± 0.014) as compared to sham lesion levels (0.410 ± 0.038; one-way ANOVA followed by Bonferroni's Multiple Comparison, $p<0.05$), which represents a 74% loss. Meanwhile, 6-OHDA rats treated with DCS exhibited only a 44% loss, which was significantly different from non-treated rats (6-OHDA+DCS CI 0.230 ± 0.061, 6-OHDA CI 0.106 ± 0.014, $p<0.05$, Bonferroni's Multiple Comparison, Fig. 2.10c, middle panel). 6-OHDA lesioning also resulted in severe loss of dopaminergic neurons from the SNc. Neuronal cell count depletion (expressed as % of sham control cell count) was significantly higher in non-treated rats [(93.32 ± 1.62)%, n=8] as compared to DCS treated [(87.43 ± 1.95)%, n=6] animals ($p<0.05$, t-test, Fig 2.10c, bottom panel).

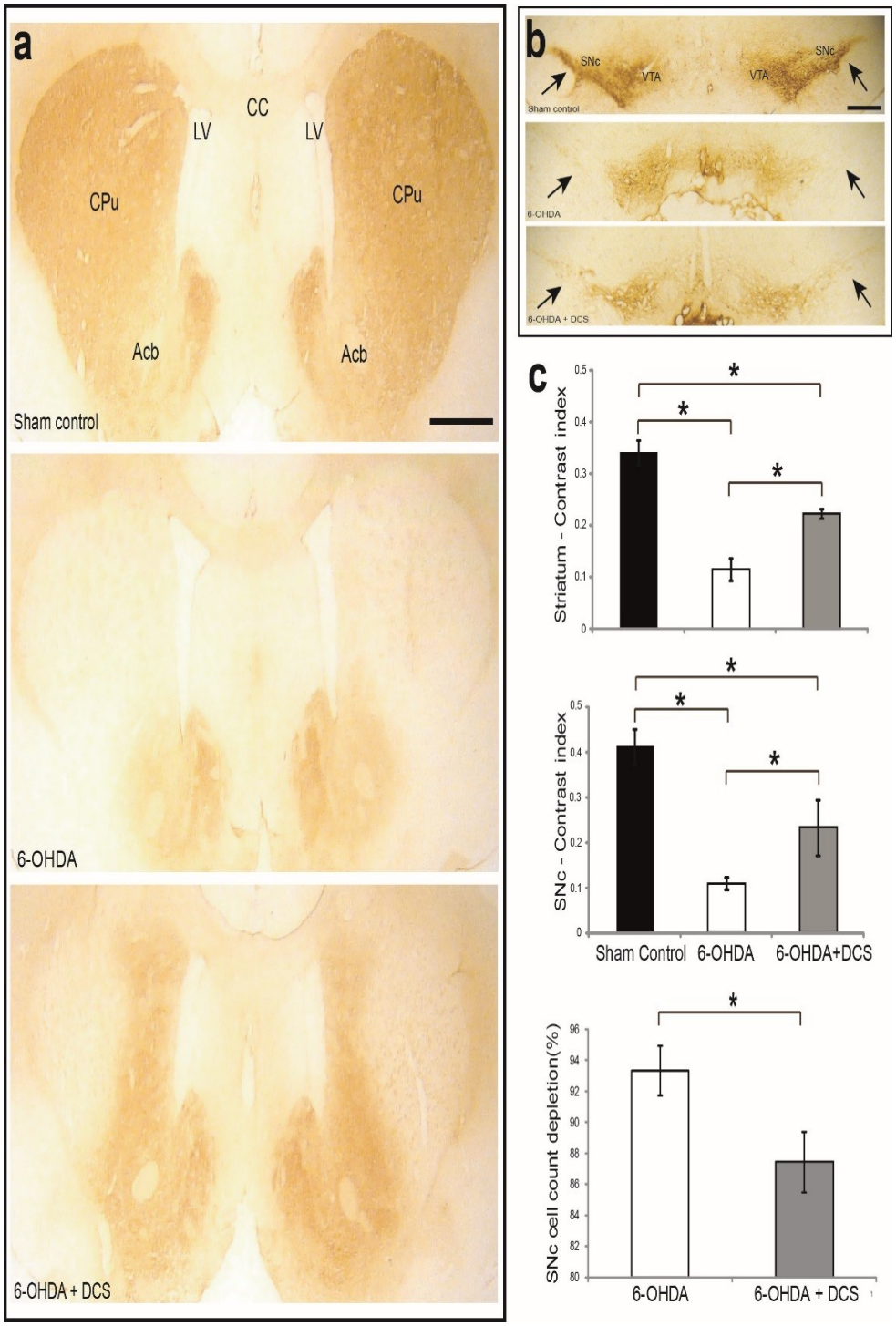
a
CC
LV
LV
CPu
CPu
Acb
Acb
Sham control
6-OHDA
6-OHDA + DCS
b
SNc
VTA
VTA
SNc
Sham control
6-OHDA
6-OHDA + DCS
c
Striatum - Contrast index
SNc - Contrast index
Sham Control
6-OHDA
6-OHDA+DCS
SNc cell count depletion(%)
6-OHDA
6-OHDA + DCS

Figure 2.10: DCS protects nigrostriatal dopaminergic system. a) Representative immunostaining for tyrosine hydroxylase (TH) in striatum (DAB stain). Note the higher dopaminergic innervation in the striatum (CPu, Acb) of DCS treated rat as compared to non-treated, scale bar = 1mm, CC = Corpus Callosum, LV = Lateral Ventricle, CPu = Caudate Putamen, Acb = Nucleus Accumbens. 6-OHDA lesion caused a 67% decrease of striatal TH levels (measured by contrast index), with respect to the sham control group, while treatment of the 6-OHDA lesioned rats with DCS resulted only in a 35% decrease, (top panel, c). The difference between the TH levels of 6-OHDA and 6-OHDA+DCS groups was significant (*:p<0.05, Bonferroni's Multiple Comparison, n=6/6). b) Representative immunostaining for tyrosine hydroxylase in substantia nigra pars compacta (SNc), scale bar = 500um, SNc = substantia nigra pars compacta, VTA = ventral tegmental area. 6-OHDA lesion resulted in a severe loss of TH immunoreactivity (measured by contrast index) in the SNc. 6-OHDA rats showed 74% loss in TH CI as compared to sham controls while DCS treated rats showed only 44%. There was significant difference between the TH levels of 6-OHDA and 6-OHDA+DCS groups in the SNc (*:p<0.05, Bonferroni's Multiple Comparison, n=6/6), middle panel, c. Dopaminergic neuronal cell loss in SNc (expressed as % of neuronal count in sham controls) was significantly higher in 6-OHDA (93.32 ± 1.62, n=8) rats as compared to 6-OHDA+DCS (87.43 ± 1.95, n=6) rats (*:p<0.05, t-test, 2 tailed). All error bars are s.e.m.

2.4.4 Global effects of neuroprotection

We also investigated the potential relation between body weight and multiple motor symptoms by calculating the linear correlations between them. This analysis revealed a positive correlation between weight and major body axis length (Spearman test: $r = 0.6639$, $p<0.0001$, Fig 2.11a).

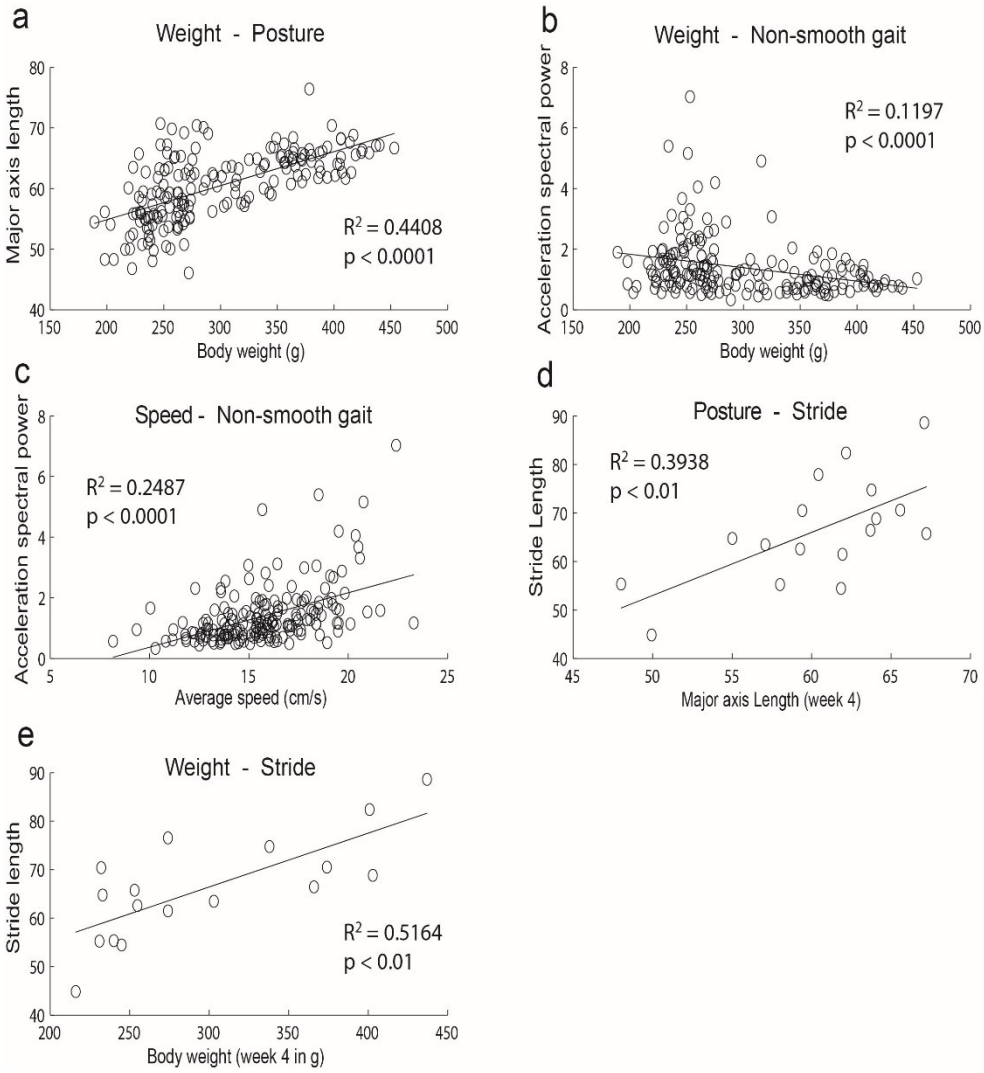

Figure 2.11: Neuroprotective effect of DCS on weight and PD symptoms. a) There was significant correlation between weight and major axis length (measure of posture) throughout the experiment (Spearman test, $p<0.0001$). b) Body weight had a significant negative correlation with spectral power of acceleration vector (indicating jerky non-smooth locomotion) – Spearman test, $p<0.0001$. c) Spectral power of acceleration vector and speed were significantly correlated throughout the experimental period (Spearman test, $p<0.0001$). Stride length measured at week 4 had significant correlation with major axis length (d, Spearman test, $p<0.01$) and body weight (e, Spearman test, $p<0.01$) indicating that recovery of body weight was related to an overall improvement in motor symptoms.

Likewise, a significant negative correlation was found between weight and non-smooth gait (Spearman test: $r = 0.346$, $p<0.0001$, Fig 2.11b), indicating that rats with greater weight loss had severe motor symptoms. Body weight also exhibited a significant correlation with stride length measured at week 4 (Spearman test: $r = 0.7186$, $p<0.01$, Fig 2.11e), indicating that an improvement in body weight was correlated with an improvement in posture and gait. There was a strong correlation between non-smooth gait and speed (Spearman test: $r = 0.4987$, $p<0.0001$, Fig 2.11c), confirming our claim that the non-smooth gait was predominantly observed during high speed displacement. A significant correlation between major body axis length and stride length (Spearman test: $r = 0.6275$, $p<0.01$ Fig 2.11d) was also observed, indicating that rats with better posture had improved gait at the end of the experimental period. Overall, all these linear correlations supported our contention that chronic DCS treatment improved the clinical effects of 6-OHDA lesions in rats.

Finally, we performed a cluster analysis using the principal component scores derived from a set of motor variables (posture, non-smooth gait, distance and speed at week 5.5, stride at week 4), histological variables (TH immunoreactivity of striatum and SNc, and SNc cells/slide) and weight at day 42. The cluster analysis correctly grouped and isolated the data points from the 6-OHDA rats but failed to separate the control and the 6-OHDA+DCS treated rats (Fig. 2.12a). Next, using only the motor variables (speed, distance, posture, non-smooth gait), we analyzed how the three groups of animals behaved over time, by plotting the progression of the first two principal components which account for 79% of the total variance. This analysis revealed that, immediately after the lesion, the

DCS treated group initially clustered together with the 6-OHDA lesioned group. Yet, 1.5 weeks afterwards, the DCS treated group started to separate from the lesioned group and move towards the control group.

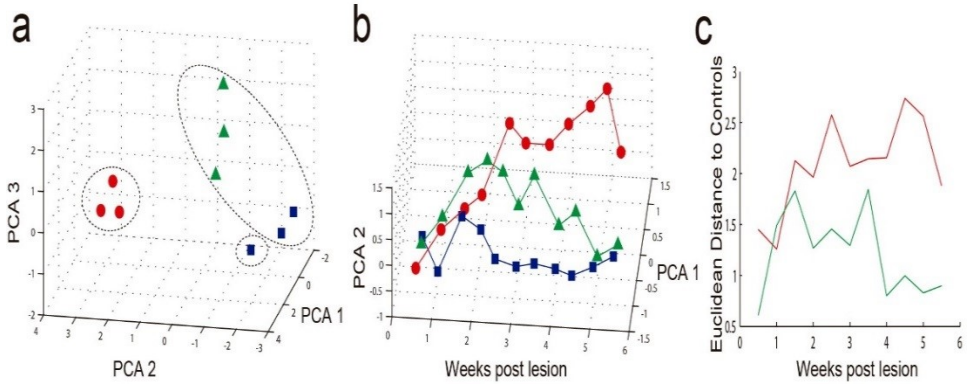

Figure 2.12: DCS reverts weight, behavioral and cellular parameters back to normality. a) Principal component analysis (PCA) was performed using 9 rats having all the data variables at a single time point at the end of the experiment [weight (day 42); axis length, acceleration power, distance and speed at week 5.5; stride (week 4); TH immunoreactivity of striatum and SNc and SNc cell count). Representation of the individual rat data points, using the first three PCs on a 3D space, shows that the rats tend to cluster according to their experimental group. Agglomerative cluster analysis of the data (dotted ellipsoids) correctly identified the 6-OHDA rats (red dots), but failed to separate the control (blue squares) and the 6-OHDA+DCS (green triangles) rats. b) PCA was performed with four motor parameters [speed, distance, non-smooth gait (acceleration power), and posture (axis length)] for all time points and the first two PC scores of all groups were averaged for each time point and plotted against time post lesion. The resulting graph shows the progression of the groups throughout the 6 weeks of the experiment. While the three experimental groups start close to each other (week 0.5-1.5), the 6-OHDA and 6-OHDA+DCS groups split from control after week 2. By the end of the experimental time, the 6-OHDA+DCS group joins the control group c) Euclidean distances of the average PCs of each group shows that the motor parameters of the 6-OHDA+DCS group started to drift from the untreated 6-OHDA group after week 1.5 and became close to control parameters after week 4.

By the end of the experimental period (week 6), the 6-OHDA+DCS group joined the control group's space and became indistinguishable from it (Fig. 2.12b). This effect can be clearly documented by plotting the Euclidean distances of 6-OHDA and 6-OHDA+DCS groups from the control group against time (Fig 2.12.c). At week 1.5 the 6-OHDA+DCS group separates from 6-OHDA and starts approaching the control's trajectory, reaching it by week 4.

2.5 Discussion

In this study we quantified for the first time the long-term effects of electrical stimulation of the dorsal column of the spinal cord (DCS) on body weight, motor symptoms and survival of nigrostriatal dopaminergic neurons in a chronic rat model of Parkinson's disease. We found that chronic DCS applied on a regular basis was associated with progressive improvement in characteristic PD motor symptoms and accelerated recovery of lost weight. This improvement in clinical signs was paralleled with the maintenance of a higher density of dopaminergic innervation in the striatum and neuronal cell count in the SNc of DCs-treated rats when compared to a group of untreated 6-OHDA lesioned animals. These results show that long-term DCS is associated with functional and structural recovery in a classic animal model of PD, suggesting that this method may be considered in the future as a potential therapy for PD patients.

Comparison between the three groups of animals utilized in this study - sham control, 6-OHDA, and 6-OHDA+DCS - revealed a progressive weight increase in

the control and the chronic DCS groups after the initial procedures (sham lesion and 6-OHDA lesion respectively). The control group reached its initial weight within 2 weeks post-surgery, as expected (Lenard *et al.*, 1991; Roedter *et al.*, 2001; Ferro *et al.*, 2005). Afterwards, this group presented a normal weight increase of approximately 3% per week. Animals treated with chronic DCS showed a weight increase of 6% per week, following the 6-OHDA lesion, which was more prominent after 2 weeks of treatment. It is not clear if the increase was only an effect of improved motor function (i.e. restoring the ability of the animal to feed itself) or increased appetite (due to overall effects of treatment) or both. For example, dysphagia caused by oropharyngeal dysfunction and hyposmia, which could be responsible for weight loss, are common findings in advanced PD patients (Ondo *et al.*, 2000; Muller *et al.*, 2001). It is also suggested that neuroendocrinological dysregulation or lower concentrations of orexins could play an important role in the feeding behavior of PD patients (Bachmann & Trenkwalder, 2006). Consistent with our present findings, data from advanced PD patients subjected to subthalamic (STN) DBS shows increased appetite and an average weight gain of 13% within ~16 months of treatment (Moro *et al.*, 1999), weight gain of 9.7 ± 7 kg within 12.7 ± 7.8 months with 60% improvement in UPDRS-III motor scores (Macia *et al.*, 2004) and a positive correlation between motor symptom improvement and weight gain (Gironell *et al.*, 2002). Our findings indicate that this latter correlation was also obtained when DCS was applied to our PD animals. Future studies in our laboratory will address how the activity of neural ensembles controlling motor and feeding functions is affected in Parkinsonian states.

The 6-OHDA lesion did not cause quantitative decrease in the animal's average speed and traveled distance. This could be explained by the phenomenon known as starvation-induced hyperactivity (Pirke *et al.*, 1993), which may have masked or compensated for the expected hypokinetic symptoms. Yet the lesioned animals exhibited clear motor symptoms, such as crouched posture, short strides, and non-smooth displacement across the open field, all of which were significantly reduced by the DCS treatment delivered only twice a week. Using the current protocol for deep brain stimulation (DBS) as a benchmark, one can postulate that a more frequent treatment or even continuous DCS could very likely lead to even larger motor effects.

At this point it is important to mention what mechanisms could account for the motor effects of DCS in PD. Both experimental evidence and modeling, obtained to explain the mechanism of DCS to treat chronic pain conditions, indicate that electrical stimulation delivered in the dorsal epidural space, as we did in the current work, activates mainly the superficial fibers of the dorsal columns and the dorsal roots of the corresponding spinal segment (Holsheimer, 2002). Thus, the consensus reached by this literature proposes that the mechanisms underlying the DCS effects reported here should emerge from the exclusive activation of ascending somatosensory fibers running through the dorsal potion of the spinal cord. This activation could, in turn, modulate the activity of multiple supraspinal structures, including thalamic, striatal and cortical areas (Fuentes *et al.*, 2009; Aguilar *et al.*, 2011). We should, therefore, emphasize that even though higher DCS intensities can additionally recruit deeper structures of the dorsal columns, such as the corticospinal tract (CST) (which in rodents is located in the ventral part of the dorsal

columns) we never observed any sign, such as muscle twitching of proximal or distal myotomes, that could support the thesis that the CST was recruited by our experimental protocol to stimulate the spinal cord. Even in humans, where CST are located more laterally, DCS at intensities above therapeutic levels can recruit fibers of the CST or local spinal motorneurons or interneurons (Nashold *et al.*, 1972; Dimitrijevic *et al.*, 1980). However, since our experiments were conducted at a stimulation intensity that did not cause any muscle twitching, it is highly unlikely that activation of CST has contributed in any way to the effects described hereby. Yet, given the anatomical differences between rodent and primate nervous system (i.e. position of the CST within the spinal cord (Kaas *et al.*, 2008)) it is crucial to confirm these results in non-human primate models. To address that very issue, our collaborators have recently concluded a series of studies showing that DCS produces the same beneficial effects, in terms of improvement of motor symptoms, in a primate model of PD (Santana *et al.*, 2014).

Degeneration of the nigrostriatal dopaminergic system is a common finding in postmortem studies of PD patients, and also a good indicator of the stage of the disease (Kish *et al.*, 1988). After long term treatment with DCS twice a week, we found that 6-OHDA rats exhibited a moderate yet significant reduction in the depletion of striatal TH-staining and TH-IR neuronal cells in SNc, as compared to non-treated lesioned animals. Although the mechanisms underlying such a reduction in dopaminergic degeneration have not been determined, we think they might be mediated by increased production or delivery of neurotrophic factors. Previous studies have shown that intrastriatal injections of brain derived neurotrophic factor (BDNF) can attenuate the effect of 6-OHDA lesions (Shults *et*

al., 1995; Klein *et al.*, 1999). A recent study involving STN-DBS has shown proof of a neuroprotective effect on the SNc neurons in a rodent 6-OHDA model (Spieles-Engemann *et al.*, 2010b), while subsequent experiments from the same group showed an increase in levels of nigrostriatal BDNF following STN DBS (Spieles-Engemann *et al.*, 2011). This could be the case with our DCS treated animals. Although clinical studies conducted with advanced PD patients to measure disease progression using 18F-fluorodopa PET failed to confirm a neuroprotective effect of clinically effective STN-DBS (Hilker *et al.*, 2005), it would be interesting to investigate in the future whether neuroprotective effects of chronic DCS can be observed in a clinical population.

Considering the increased longevity of the population worldwide, the introduction of novel treatments that address both the symptoms and progressive nature of PD constitute a major priority for the management of Parkinsonian patients. Based on recently described preliminary evidence showing efficacy of DCS in a series of PD patients worldwide (Agari & Date, 2012; Fenelon *et al.*, 2012; Landi *et al.*, 2012; Hassan *et al.*, 2013a) and our own results in both acute and chronic PD animal models, we propose that chronic epidural DCS, a procedure that does not invade the brain, does not have serious side effects and can be carried out at much lower costs and risks for patients, could be employed at the early clinical stages of PD to manage some of its cardinal motor symptoms. This conclusion is further supported by recently published results showing that DCS can also alleviate motor symptoms in a primate model of PD (Santana *et al.*, 2014).

At this point, there are very few reports of DCS in PD patients. Thus, it is difficult to predict if the eligibility of DCS will be substantially better than for DBS. However, the

lack of major side effects, the relative ease with which the surgical procedure can be performed and the fact that there is no need to penetrate into brain tissue suggest that DCS could become an early stage therapy in the future management of PD patients.

3. Dorsal Column Stimulation for Artificial Tactile Sensation

3.1 Abstract

Dorsal column stimulation (DCS) is an effective therapy for a number of neurological conditions, including Parkinson's disease and spinal cord injury. Although DCS has been used to treat chronic pain in the clinic for decades, its full potential has not been realized. In particular, there has been no implementation showing DCS as a channel to communicate with the brain. Here we explored DCS as a technique to transmit artificial somatosensory information to the cortex and trained rats to discriminate up to four artificial tactile sensations induced by DCS. We observed that artificial tactile information delivered by DCS was encoded in multiple brain areas and the encoding changed as the animals learnt the discrimination task. Our results suggest that DCS can be used in the future to send prosthetic somatosensory information to the brain in order to incorporate novel artificial senses or provide feedback from a brain machine interface.

3.2 Introduction

Brain machine interfaces have shown promise for the treatment of neurological impairment and limb loss by transforming neuronal activity into commands that control artificial actuators like cursors, robotic devices and prosthetic limbs (Chapin *et al.*, 1999; Carmena *et al.*, 2003; Lebedev & Nicolelis, 2006; Nicolelis & Lebedev, 2009). The role of

tactile feedback is most important for efficient control of actuators and various locations along the afferent sensory pathway have been studied for creating artificial sensations right from the periphery using targeted nerve innervation (Marasco *et al.*, 2009) to Intracortical Microstimulation (ICMS) of the somatosensory cortex (Weber *et al.*, 2012). Studies have shown that ICMS of area 3b and 3a of the somatosensory cortex (S1) can be used respectively for creating a sense of flutter (Romo *et al.*, 1998; Romo *et al.*, 2000) and proprioception (London *et al.*, 2008) respectively in monkeys. Thalamic stimulation has a been used to induce somatotopically organized percepts in humans (Heming *et al.*, 2010) and work pioneered by (O'Doherty *et al.*, 2011; O'Doherty *et al.*, 2012) has also demonstrated the use of ICMS of S1 as a site for tactile feedback in a brain machine interface involving rhesus monkeys. However, surprisingly, there has been no attempt to use DCS, for providing tactile feedback or creating discriminable percepts in humans or animals. Although, spinal cord stimulation has been used for the treatment of chronic pain for decades, its role as a channel to deliver tactile information to the cortex has never been explored before (Compton *et al.*, 2012). This could be because most patients with spinal cord injuries are unable to sense their bodies below the level of injury deeming the spinal cord non-functional for afferent transmission of signals.

However, recently it has been shown that spinal cord stimulation has considerable promise for the treatment of Parkinson's disease and spinal cord injury (Agari & Date, 2012; Fenelon *et al.*, 2012; Landi *et al.*, 2012; van den Brand *et al.*, 2012; Hassan *et al.*, 2013b). While the therapeutic effect of DCS for spinal cord injury has been reported to be based on modulation of local spinal circuits (Linderoth & Foreman, 1999; D'Mello &

Dickenson, 2008), our laboratory has shown that alleviation of Parkinsonian symptoms is facilitated by direct modulation of corticostriatal circuits (Fuentes *et al.*, 2009; Santana *et al.*, 2014) and a neuroprotective effect is responsible for long term rescue of dopaminergic neuronal cell loss (Shinko *et al.*, 2014; Yadav *et al.*, 2014). These findings suggest that the dorsal columns of the spinal cord can be used as a channel to modulate neuronal activity and communicate with the brain.

To test the hypothesis that DCS can be used as an effective technique for communicating with the brain, we trained mildly water deprived rats to discriminate up to four artificial tactile sensations delivered as DCS patterns in order to obtain a water reward. We analyzed how the encoding of these artificial percepts changed between early and late phases of training by processing the neuronal spiking activity through a decoding algorithm and predicting the classification accuracy of the neural data.

Our demonstration opens up new possibilities for using the spinal cord as an information highway to transmit both therapeutic as well as somatosensory information to the brain, in patients with spinal cord injury or those suffering from neurological disorders. DCS, a semi-invasive, easy to perform procedure can have wide ranging clinical application in areas such as BMI neurofeedback for motor rehabilitation, prosthetic somatosensation and in general for expanding the sensory repertoire of human perception.

3.3 Methods

3.3.1 Artificial Tactile Discrimination task using DCS

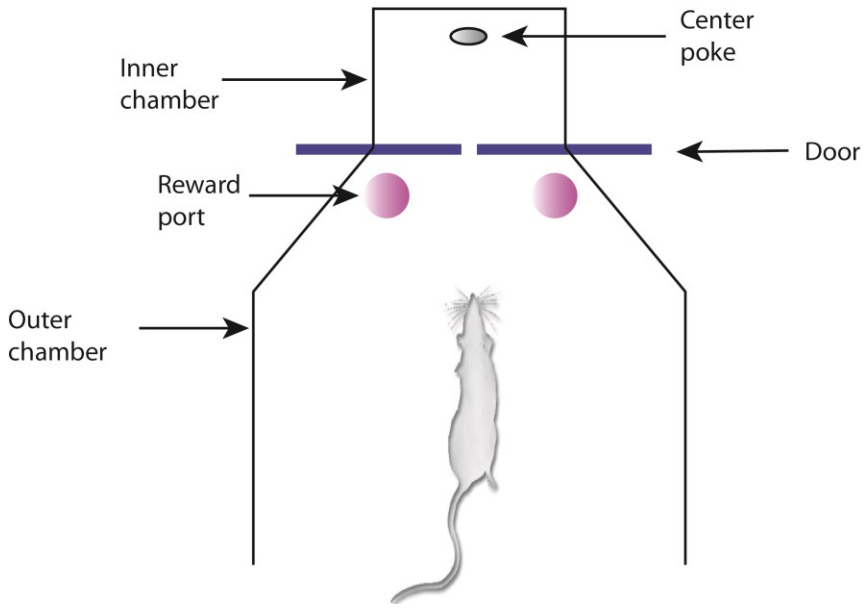

Figure 3.1 Schematic of Artificial Tactile Discrimination Behavioral Training Box. Inner and outer chamber are separated by a sliding door. Once the trial begins, the door opens and rat has to make a nose poke in the center of the front wall in the inner chamber. As it passes through inner chamber DCS is initiated. 'Virtual Narrow' tactile sensation (101 pulses) is rewarded with water reward in the left reward port while 'Virtual Wide' (1 pulse) in the right. After the center poke, rat has to come out and make a response in the reward port associated with the stimulation pattern. Incorrect responses are not rewarded.

Moderately water deprived rats (n=12) were trained to discriminate DCS induced tactile sensations using modified version of aperture width tactile discrimination behavioral box where the discrimination bars weren't used and pulled back to maximum width (Fig 3.1). After undergoing basic training that included entering inner chamber, center poke in front wall, poking left or right reward port, rats were trained to discriminate between a train of 100 pulses delivered at 333 Hz associated with a correct response in left reward port and 1 pulse corresponding to a correct response in right reward port. DCS was initiated only when rats crossed the photobeam, before the center poke, in the inner chamber. The

artificial tactile sensation with 101 pulses and 1 pulse was named 'Virtual narrow' and 'Virtual wide' respectively. Correct responses in respective reward ports were rewarded with 50ul water. After ~10 training sessions, a stable performance of >80% was achieved. In 6 rats, neuronal single and multi-unit and local field potential signals were recorded from multiple areas ([4 rats: M1, S1 and STR]; [1 rat: M1 and S1]; [1 rat: S1]) as they learnt to discriminate DCS patterns over 11 sessions.

3.3.2 Discriminating 3 and 4 artificial tactile stimulation patterns

2 rats that were previously trained to discriminate stimulation patterns associated with 'virtual narrow' and 'virtual wide' sensations were trained to discriminate 3 different DCS patterns. An additional reward port was installed in the behavioral box that corresponded with the 3rd stimulation pattern (100 pulses at 100 Hz). Initially, rats failed to associate 3rd reward port with 3rd stimuli pattern, thus, to habituate them with the new reward port, we used a unique training paradigm (Fig 3.2, right). First, the novel stimuli was incorporated in the sensory perception of the rats in Stage I by rewarding them when they made a response in the novel reward port. Once the rats successfully learnt to associate the novel stimulation pattern with the new reward port, previously trained stimulation patterns were paired with the 3rd stimuli (2 unique combinations, stage II and III). After the rats reached performance criteria (>60%) in stages II and III, all 3 stimuli were simultaneously introduced in the same session to begin the actual 3 stimuli discrimination task. Performance was analyzed based on percentage of correct trials for entire session and also % correct trials for each stimuli type.

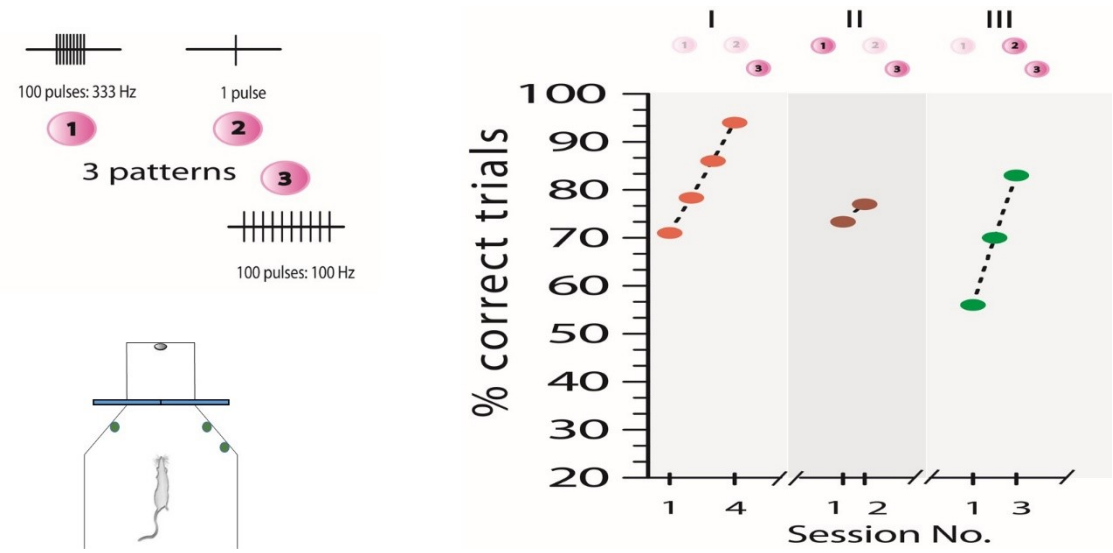

Figure 3.2 Training paradigm for teaching rats to discriminate 3rd novel stimuli. Left-top: 3 stimulation patterns, left-bottom: Behavioral box with 3 reward ports. Right: In stage I, 3rd DCS pattern (100 pulses at 100Hz) is introduced, in Stage II and III, 3rd pattern is paired with previously learnt patterns 1 and 2. Once rats perform >60% correct in stages II and III, all 3 patterns are simultaneously introduced.

Thereafter, 1 rat was trained to discriminate 4 different DCS patterns (4th stimuli consisted of 100 pulses delivered in 5 bursts of 20 pulses each with inter-burst frequency of 2 Hz and inter pulse frequency of 333 Hz (Fig 3.3). Similar to previous training paradigm, first, the 4th novel stimuli was incorporated into the sensory perception of the rat (stage I), followed by 3 unique combinations of previously learnt stimuli with the 4th stimuli, stages II, III and IV). Once the rat performed at criterion (>60%) at each stage, all 4 stimuli were introduced in the same session. Performance was analyzed based on percentage of correct trials for entire session and also % correct trials for each stimuli type.

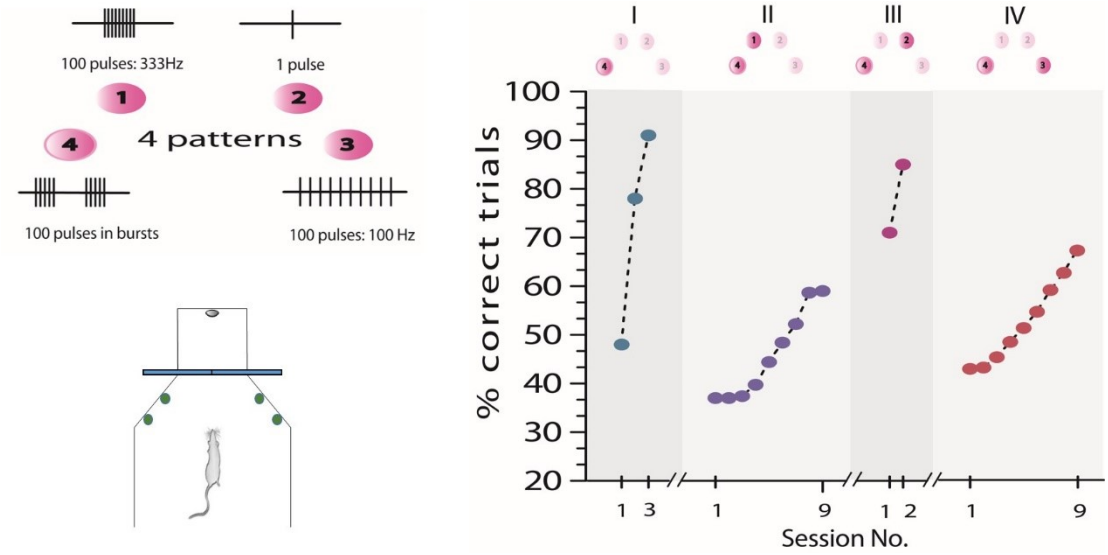

Figure 3.3 Training paradigm for teaching rats to discriminate 4th novel stimuli. Left-top: 4 stimulation patterns, left-bottom: Behavioral box with 4 reward ports. Right: In stage I, 4th DCS pattern (100 pulses in burst) is introduced, in Stage II and III and IV, 4th pattern is paired with previously learnt patterns 1, 2 and 3. Once rats perform >60% correct in stages II and III and IV, all 4 patterns are simultaneously introduced in a session.

Irrespective of the stage of learning (novel stimuli, pairs of combinations or all stimuli together), chance performance was maintained at either 33% (learning 3 stimuli) or 25% (learning 4 stimuli) by opening all rewards port after the center nose poke, thereby keeping the probability of correct response by chance at a minimum. This unique method made the learning task harder for the rats and allowed us to study how the performance on previously learnt sensations changed while incorporating a novel stimuli into the animal's sensory perception.

3.3.3 Surgery for implantation of DCS electrode and microelectrode array

Custom built movable microelectrode bundles or fixed arrays were implanted in the M1, S1 and striatal areas of 6 rats trained on the 'Artificial Tactile Discrimination using DCS' task (Fig 3.4).

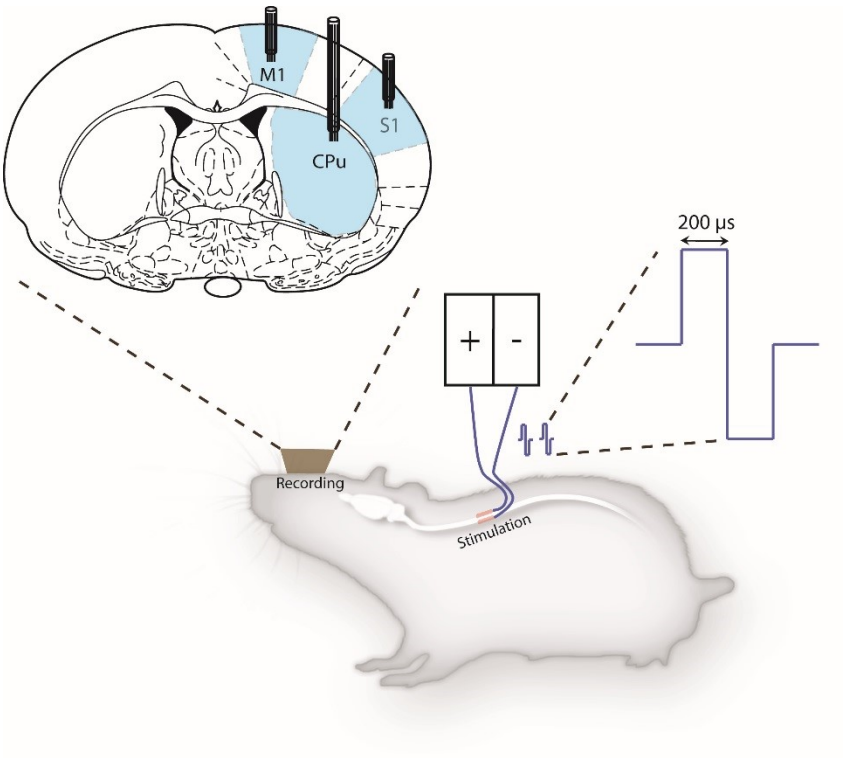

Figure 3.4 Rat with stimulation and recording electrodes. Multielectrode arrays were implanted in M1 (motor cortex), S1 (somatosensory cortex) and STR (striatum denoted by CPu). Bipolar DCS electrodes were implanted in the epidural space between T2 vertebra and the spinal cord and connected to an electrical microstimulator, controlled by custom Matlab scripts.

The stereotaxic coordinates for each of the areas relative to bregma in mm are : M1 [AP: 0 mm; ML: 1.6 mm; DV: -1 mm], S1 [AP: -3 mm; ML: 5.5 mm; DV: -1.25 mm], STR [AP: 0 mm; ML: 3.5 mm; DV: -4.5 mm]. Out of 6 rats that were implanted with

recording electrodes; 2 rats had bilateral M1 and STR but unilateral S1 electrode in left hemisphere; 2 rats had unilateral M1, S1 and STR electrodes in left hemisphere, 1 rat had unilateral M1 and S1 electrode in left hemisphere and 1 rat had unilateral S1 electrode in left hemisphere. Bipolar dorsal column electrodes were implanted in the epidural space between T2 vertebra and spinal cord as explained in previous chapter (see methods, chapter 2)

3.3.4 Neurophysiological recording

Neuronal data was sampled from the recording electrodes at 40 KHz using a Multichannel Acquisition Processor (Plexon Inc., Dallas, TX). Single and multi-units were sorted online using (SortClient 2002, Plexon Inc., Dallas, TX) and interfaced with Matlab (8.4.0, Mathworks, Natick, MA) for real-time analysis and classification.

3.3.5 Dorsal column stimulation

DCS consisted of charge balanced biphasic square pulses of 200 μsec duration delivered at 100-333 Hz, either as 'trains' or 'bursts' of pulses depending on the condition of the experiment. Stimulation intensities were determined during each session and set at a value between sensory and discomfort threshold (therapeutic range with intensities that varied from 110 μA to 600 μA). To identify optimum stimulation intensity, initially, 'paresthesia threshold' was identified by the animal's whisking response to stimulation and subsequently intensity was increased until a point a muscle twitch was seen, i.e. 'discomfort threshold'. Stimulation intensity was kept much lower than the discomfort

threshold. Whenever, intensity was higher than the discomfort threshold, rats stopped performing the task and if intensity was below the paresthesia threshold, their discrimination accuracy dropped to chance levels. Specific patterns of stimulation pulses were generated by custom scripts written in Matlab (8.4.0, Mathworks, Natick, MA) that instructed an electrical microstimulator (Master 8, AMPI, Jerusalem, Israel).

3.3.6 Neural decoding algorithm

To analyze the changes in neuronal activity as the rats learnt to discriminate 'virtual narrow' and 'virtual wide' trials, single and multi-unit activity was sampled for 100 msec after the end of stimulation trains (to prevent the effect of stimulation artifact). Spiking data was binned in 25 msec bins and each data bin of each neuron was considered as a feature for the current trial and used to predict the number of pulses using a logistic regression learning algorithm (Fig 3.5). Binned firing rates from all previous trials were organized in the data set used to train the classifier for prediction of current trial. 'SVD' function was used to reduce the dimensionality of features such that 99% of variance was retained in the data set. A 'gradient descent' approach with regularization parameter set at 1 was implemented using the 'fminunc' function to minimize the regression cost function. All scripts were custom written in Matlab (8.4.0, Mathworks, Natick, MA) using in house functions. Because the classifier was updated on every single trial based on data from all previous trials, the logistic transformation weights changed throughout the session.

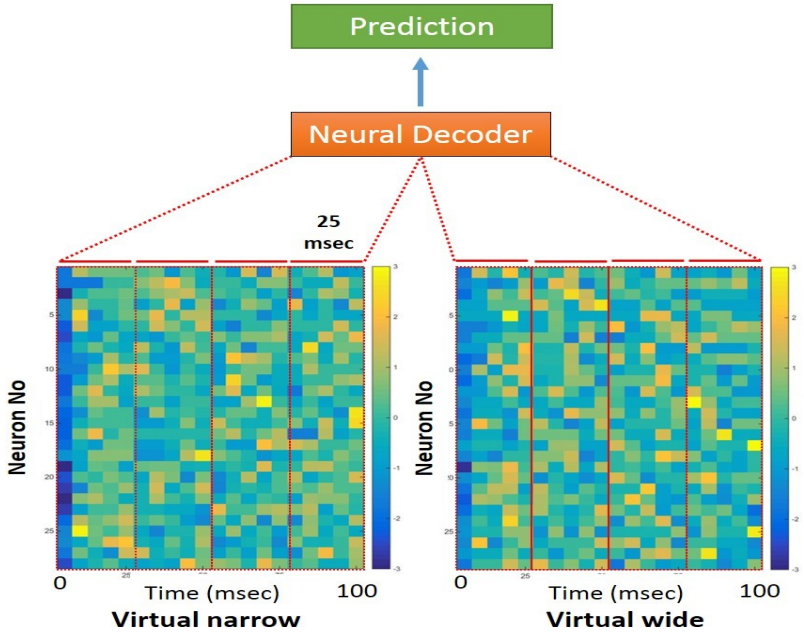

Figure 3.5 Neural decoding strategy for classification of trials. Representative firing rates (z-scored) of neurons for 'virtual narrow' and 'virtual wide' trials in one session. Firing rates were binned in 25 msec bins and sent to a neural decoder for classification of trials using a logistic regression learning algorithm.

3.3.7 Data Analysis

Percentage correct trials was used to assess behavioral performance of all rats. Performance of decoding algorithm was measured by calculating the percentage of trials correctly predicted from entire session. Prediction error was calculated as mean squared error of expected value from predicted value using all trials from the session. Comparison of groups or conditions was performed using t-tests. Whenever distributions failed the normality test, non-parametric test such as Mann-Whitney was used.

3.4 Results

3.4.1 Artificial Tactile Sensation of two different stimuli using DCS

We trained rats (n=12) to discriminate artificial tactile sensations delivered to the cortex through dorsal column stimulation. Rats learnt to discriminate between two stimulation patterns (101 pulses at 100 Hz vs 1 pulse) representing 'virtual narrow' and 'virtual wide' trials in a modified version of aperture width tactile discrimination task where discrimination bars weren't used (Fig 3.1). By the 11th session rats were completely trained exemplifying mean performance of 91.75 ± 1.36 (Fig 3.6). We saw a steep increase in earlier training session (sessions 1-4) followed by a gradual increase and then another steep increase in late training (sessions 8-11).

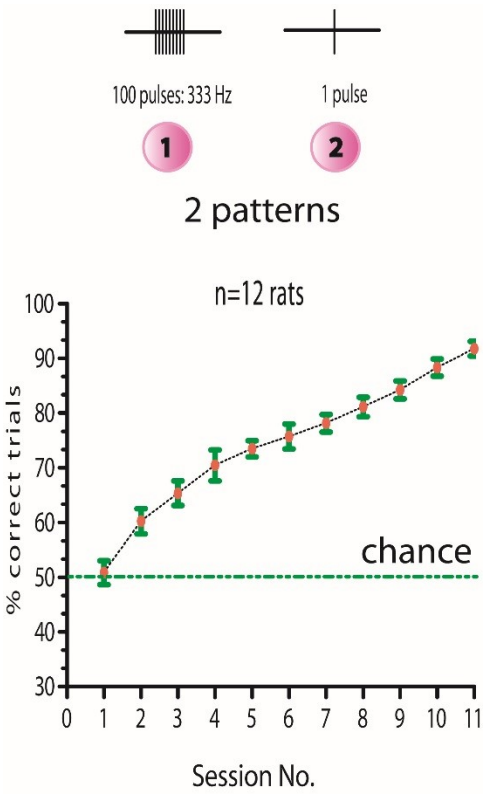

Figure 3.6 Learning curve for tactile discrimination of two DCS patterns

Analysis of performance on individual stimuli revealed that both the 'virtual narrow' (Pattern 1) and 'virtual wide' (Pattern 2) stimuli were learnt at a similar rate (Fig 3.7). Performance started around chance (50%) for both stimuli and gradually increased to >90% as the rats learnt to discriminate more accurately.

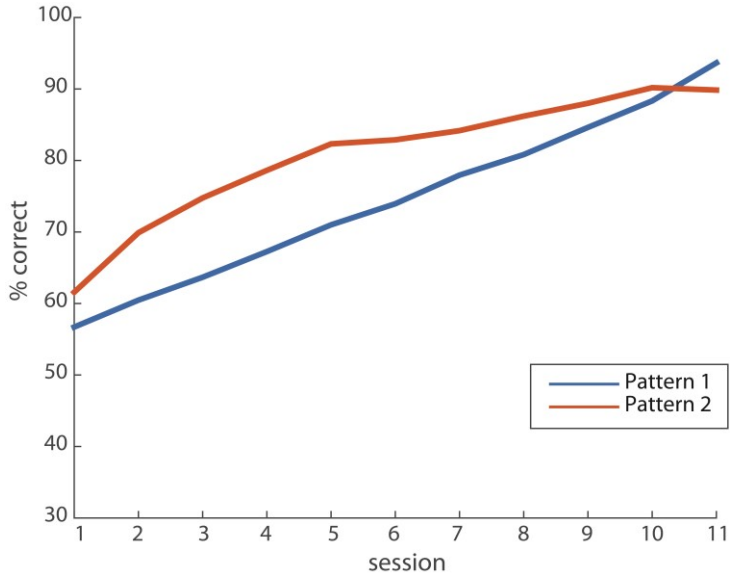

Figure 3.7 Performance of rats for each of the two stimuli across sessions

3.4.2 Plasticity associated with DCS induced learning

To examine if DCS induced learning was driven by cortico-striatal plasticity we compared behavioral performance and decoding performance of a neuronal decoding algorithm between the first (early) and last (late) training session in 5 rats that had stable single and multi-unit recordings throughout the training period. We found a significant difference in behavioral performance between early (51.2 ± 3.73) and late (92.6 ± 1.75) training sessions ($p<0.01$, Mann Whitney test, Fig 3.8a), which was consistent with a

significant difference between the performance of the neural decoder [early (74.59 ± 3.89) and late (85.57 ± 2.58), $p<0.05$, unpaired t test, Fig 3.8b]. The prediction error of the neural decoder, calculated as variance from expected value was higher for early training (0.1762 ± 0.0263) as compared to late (0.1076 ± 0.0189), ($p<0.05$, unpaired t test, Fig 3.8c) suggesting a role of corticostriatal plasticity as the animals learnt to discriminate DCS induced artificial tactile sensations.

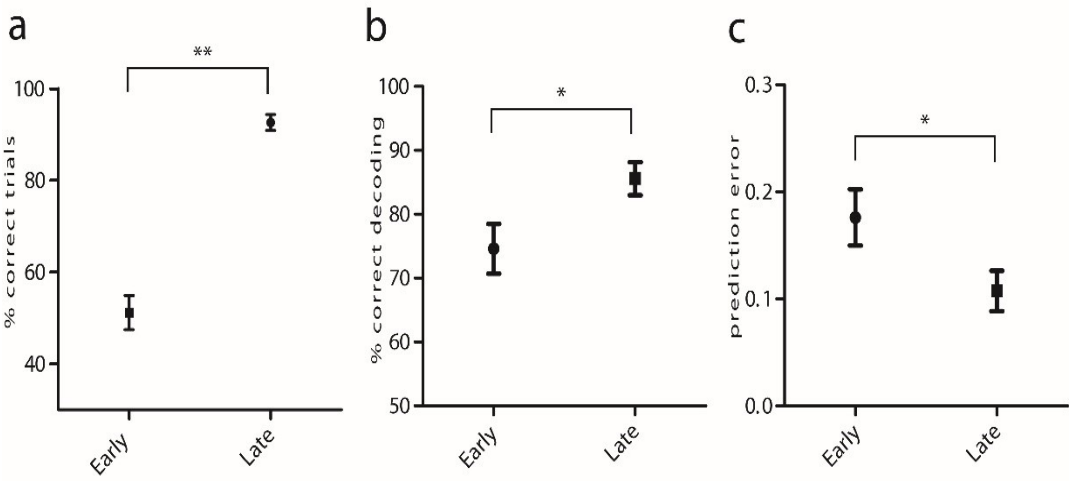

Figure 3.8 Early vs Late changes in performance and neural activity. a) Performance of rats in discriminating 100 vs 1 pulses was significantly higher in late training period as compared to early. This was corresponded by improved performance of the neural decoding algorithm (b) and also a reduction in the prediction error associated with decoding (c).

3.4.3 Discriminating 3 different DCS patterns

Next, we explored if some rats could discriminate an additional DCS stimulation pattern, associated with a new reward port, namely, 'virtual far wide'. Initially, they struggled to associate the novel stimulation pattern (100 pulses at 100 Hz) with the new reward port and were introduced to a unique training paradigm (Fig 3.2, right) where the

number of stimuli to discriminate were gradually increased, but the probability of chance response was kept constant by keeping all rewards ports accessible for a response (see methods for details).

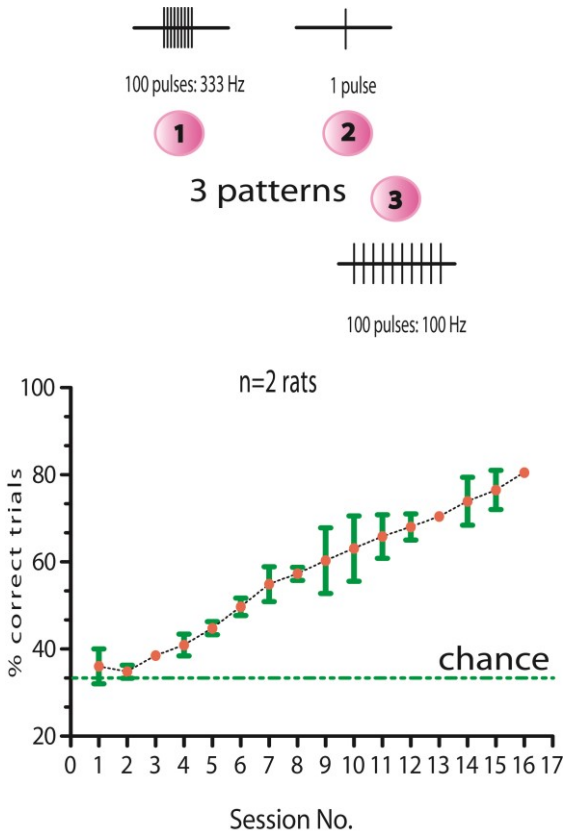

Figure 3.9 Learning curve for tactile discrimination of three DCS patterns

Once they reached performance criteria >60% in discriminating all pairs of patterns they began training where all 3 patterns were delivered in one session. Rats (n=2) successfully learnt to discriminate between 3 DCS delivered artificial tactile patterns (Fig 3.9) reaching 80% in ~15 sessions with max performance of 81%. By studying the learning performance for each of the stimuli throughout the sessions, we found that as the rats started performing better on the 3rd stimulation pattern, their performance on the 1st pattern slightly

decreased. This could be because the 2 patterns had the same number of pulses and differed only in frequency of stimulation. However, once the rats learnt to differentiate the 3rd pattern fairly accurately, their performance on both the patterns increased gradually, suggesting that once the novel stimuli was learnt, it became easier to differentiate all stimulation patterns.

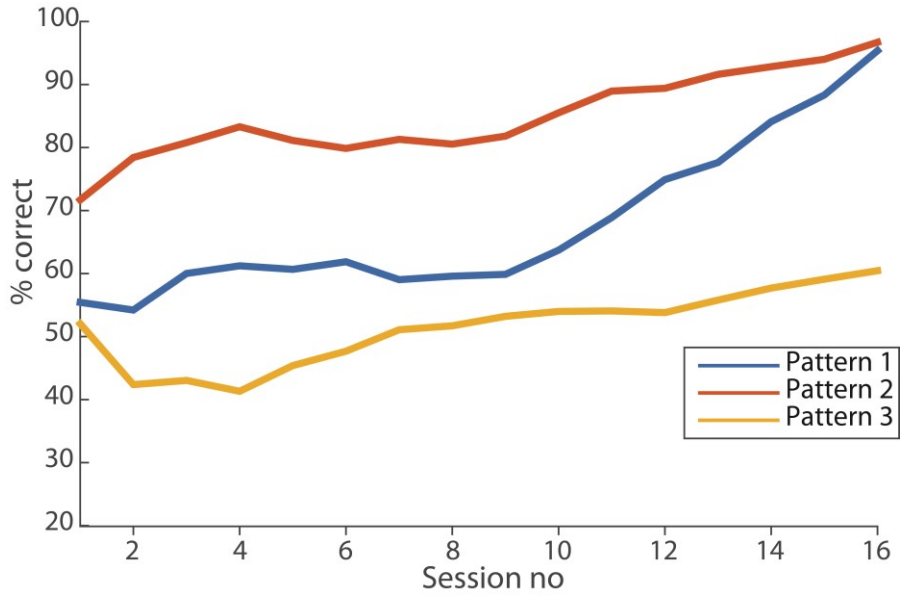

Figure 3.10 Performance of rats for each of the 3 stimuli across sessions

3.4.4 Discriminating 4 different DCS patterns

To extend the limits of DCS induced learning we added an additional reward port, namely 'virtual far narrow' associated with a novel stimulation pattern (100 pulses in bursts of 20 pulses each with inner-burst frequency of 333Hz and inter-burst frequency of 2Hz). After training to successfully discriminate 3 patterns one rat moved on to train for 4 different stimulation patterns. Initially, the rat failed to associate the novel stimuli with the

novel reward port and hence was subjected to our unique training protocol illustrated in (Fig 3.3, right). First, the rat was trained to identify 4th stimulation pattern alone, and subsequently it was paired with previously learnt 3 patterns. Once the rat performed above criterion (>60%) on all the pairs of patterns, all 4 patterns were simultaneously introduced in the session. Performance started around chance levels but gradually increased as the rat learnt the discrimination task. The best discrimination performance of 81%, significantly higher than chance levels (25%) was achieved in this paradigm (Fig 3.11) suggesting the tremendous capacity of the dorsal column pathway to serve as a channel that can transmit new sensory information into the sensory repertoire of the brain.

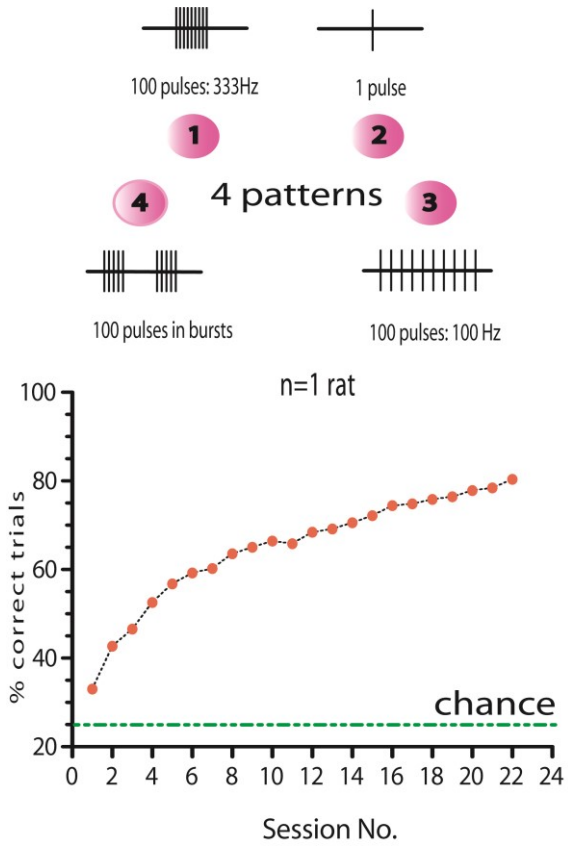

Figure 3.11 Learning curve for tactile discrimination of four DCS patterns

To understand how the 4th tactile sensation was incorporated in the rat's sensory perception, we studied the learning performance for each individual stimuli throughout the sessions (Fig 3.12). We found that performance on pattern 1 and 2 was considerably higher throughout the training period. However, as the rat started learning 4th stimulation pattern, its performance on the 3rd pattern gradually decreased, but once an equilibrium point was reached (~session 10), performance on both 3rd stimuli and 4th stimuli pattern gradually increased.

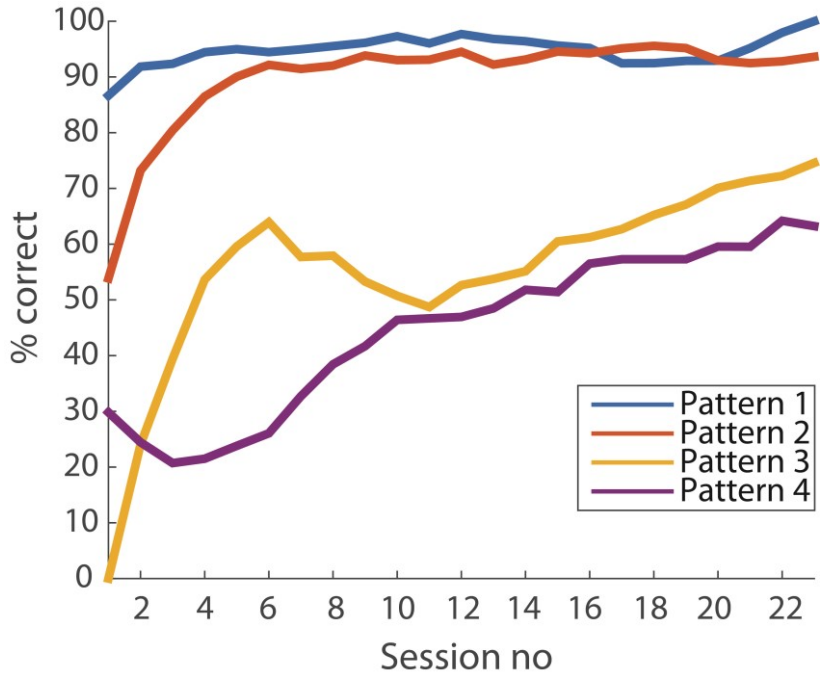

Figure 3.12 Performance of the rat for each of the 4 stimuli across session

3.5 Discussion

In our study we successfully demonstrated that dorsal column stimulation can be used as an effective technique to transmit information to the brain. We trained rats for the first time to discriminate four different artificial tactile sensations delivered as stimulation patterns through dorsal column stimulation. We found that the encoding of artificial tactile information in multiple brain areas changes between early and later phases of training suggesting a role of neuroplasticity in DCS induced learning.

To our knowledge this is the first time that dorsal column stimulation was used to generate tactile sensation in order to guide goal directed behavior. Previously it has been shown that monkeys can discriminate two different ICMS frequencies delivered in area 3a (London *et al.*, 2008) and 3b (Romo *et al.*, 1998) of the somatosensory cortex to generate artificial proprioceptive and tactile percepts respectively. It is also known that the therapeutic effect of DCS on pain symptoms is associated with the generation of paresthesia in human subjects (Holsheimer & Barolat, 1998; Holsheimer, 2002), but no study has shown that different stimulation frequencies create consciously discriminable percepts. Our demonstration of a rat that successfully discriminated between 4 different DCS induced tactile sensations proves that the spinal cord has a tremendous capacity to encode novel information in the sensory repertoire of the brain. By using a unique training paradigm where multiple patterns were paired together before the actual experiment, we were able to test 6 different pairs of stimuli. We found that the performance was lowest when stimuli pairs were associated with spatially closest rewards ports. Another study from our lab where rats learnt to respond to infrared light using ICMS has indicated similar

results where the performance decreased as the angle between the reward ports was reduced (Thomson *et al.*, 2013). This suggests that discrimination of DCS induced percepts is correlated with the spatial proximity of associated reward ports. A limitation of our study was that the stimulation intensity was constant throughout a session regardless of stimulation frequency. It is possible that varying the intensity depending on stimulation pattern and frequency might result in better discrimination accuracy and thus faster learning. In a future study, it would be interesting to use additional stimulation channels placed at different locations along the dorsal spinal cord to test if the rate of learning in discrimination of four tactile percepts can be increased by using multiple spatio-temporal patterns.

Previously, it has been shown that corticostriatal plasticity plays an important role as rats learn abstract neuroprosthetic skills (Koralek *et al.*, 2012). We also found significant improvement in the decoding performance of recorded single and multi-unit activity as rats learnt to discriminate between 100 and 1 DCS pulses. The improvement in decoding performance was paralleled by a reduction in prediction error between late and early phases of training. This suggests the role of corticostriatal plasticity associated with DCS induced tactile sensations. Future work exploring this role in more depth can reveal how artificial tactile information gets encoded in the brain.

Thus, we can conclude that the dorsal column of the spinal cord is an efficient channel to transfer artificial tactile information to the brain and DCS can have numerous clinical applications in BMI neurofeedback or prosthetic somatosensation.

4. A Brainet for Cortico-Spinal Communication

4.1 Abstract

Dorsal Column Stimulation (DCS) is an effective therapy for a number of neurological conditions, including Parkinson's disease and spinal cord injury. Although DCS has been used in clinic for decades there has been no implementation of a therapist-patient interface, where neural signals derived from a healthy brain would control stimulation applied to the spinal cord of a patient. Here we modeled such an interface using a Brainet that interconnected two rats: an encoder and a decoder. While the encoder rat performed a real or artificial tactile discrimination task, it's cortical and striatal signals were recorded, processed by a neural decoder and transmitted to the spinal cord of the decoder rat using DCS. We found that both real and artificial tactile information was encoded in multiple corticostriatal areas in the brain. Our study demonstrated for the first time a cortico-spinal communication between different organisms. The obtained results suggest that such a Brainet could be used in the future to enable a healthy brain to directly modulate neural activity in the nervous system of a patient, facilitating plasticity mechanism needed for efficient recovery.

4.2 Introduction

Brain to Brain Interfaces (BTBI) is an emerging concept which has gathered momentum in the last couple of years, where, real-time sensorimotor information is

transferred between multiple humans or animals to create dynamic interdependent systems. Although the first demonstration of this new paradigm was performed with rats (Pais-Vieira *et al.*, 2013a), subsequently, there have been displays of similar interfaces between humans (Grau *et al.*, 2014). The prompt adoption of non-invasive techniques like EEG and TMS has sped up the development of such interfaces between human subjects (Rao *et al.*, 2014). However, there has been no attempt to create a therapist-patient interface where neuronal signals from a therapist could directly modulate activity in a patient. Previously, we have shown that DCS alleviates symptoms of Parkinson's Disease in rats and monkeys (Fuentes *et al.*, 2009; Santana *et al.*, 2014; Yadav *et al.*, 2014) and that DCS can be used to encode artificial tactile information in rats (chapter 3). To converge these two ideas and initiate the creation of a therapist-patient interface, we developed a Cortico-spinal Brainet which serves as a proof of concept for the first cortico-spinal communication between two conscious organisms.

We created a real-time Brainet where tactile information sampled by whiskers of encoder rats was transmitted to the spinal cord of a decoder rat using DCS after a sigmoidal transformation. To further explore DCS as a channel for both encoding and decoding of information, we created another cortico-spinal brainet where artificial tactile information encoded through the spinal cord of encoder rats was decoded in real time from their cortico-striatal neuronal spiking activity and transmitted to the spinal cord of a decoder rat. Finally, we also studied how multiple cortico-striatal areas encode real (whiskers) as well as artificial (DCS) tactile information.

Recently, it has been shown that multiple brains of rats can be connected to create an organic computing device using ICMS as an external cue (Pais-Vieira *et al.*, 2015) or that multiple non-human primates can modulate their neuronal activities together to perform a combined arm movement task (Ramakrishnan *et al.*, 2015). This suggests that DCS can be used in experiments involving multiple brains to transfer information or provide feedback. Our successful demonstration of a cortico-spinal brainet reinforces the hypothesis that DCS can be an efficient channel for transmitting relevant information to the brain.

4.3 Methods

4.3.1 Brainet for Cortico-spinal communication

Moderately water deprived rats (n=4), 'encoders', were trained to perform an aperture width discrimination task after basic behavioral training as explained previously (Wiest *et al.*, 2010). The task involved discrimination of narrow and wide aperture widths to receive a water reward. Rats were placed in the outer chamber and waited for the door to open to enter the inner chamber (see Fig 4.1). Once inside, the rats had to pass through discrimination bars with adjustable widths in order to nose poke in the central wall. After center nose poke two reward doors opened in the outer chamber, which the rats had to lick in order to receive water reward. Depending on the width of aperture rats had to go to either ports to receive 50ul of water reward. Narrow aperture width was rewarded by the left reward port while wide aperture with right reward port. Tactile discrimination was assessed

based on the percentage of correct trials. Once rats reached performance >90%, they were ready for the brainet experiments.

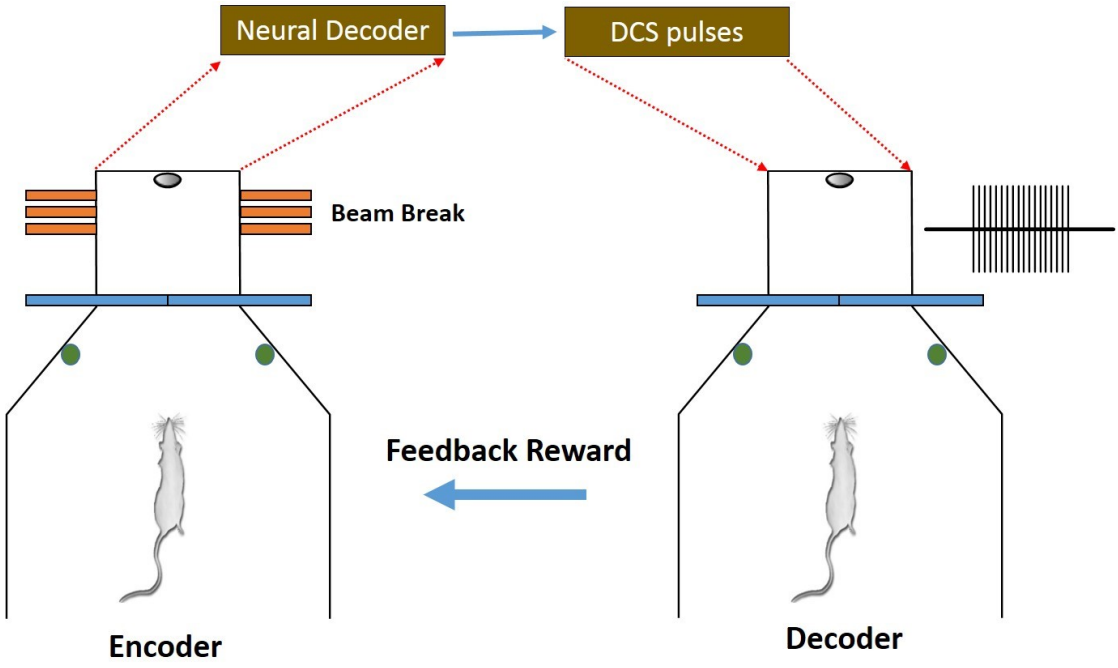

Figure 4.1 Brainet for cortico-spinal communication. Single and multi-unit activity from M1, S1 and STR of encoder rat was sent to a logistic regression classifier (neural decoder) which predicted the number of DCS pulses (between 1 and 101) to be delivered to decoder rat. If decoder predicted a correct response, the encoder rat received 2nd water reward as feedback.

Similarly, decoders (n=10) were trained to discriminate between 101 pulses at 100 Hz and 1 pulse delivered using DCS. 101 pulses were associated with the 'virtual narrow' trial which was rewarded after a response in the left reward port while 1 pulse was associated with the 'virtual wide' trial rewarded in the right reward port. Incorrect responses were not rewarded. DCS induced tactile discrimination was assessed based on

the percentage of correct trials. Once rats reached performance >80%, they were ready for the brainet experiments.

In experiment one, as encoder rats performed whisker tactile discrimination task, their cortical and sub-cortical (M1, S1 and STR) single and multi-unit activity was sent to a neural decoder (explained below) which converted it into number of DCS pulses to be applied to the spinal cord of decoder rats (Fig 4.1). The first 20 trials of cortico-spinal interface were used for training the neural decoding algorithm, where the number of pulses were either 1 for a 'wide width' trial or 101 for a 'narrow width' trial. From trial 21, the number of DCS pulses to be sent to decoder rat (between 1 and 101) were predicted based on cortical activity of encoder rat. If the decoder discriminated correctly both rats received a water reward (additional feedback reward for encoder). The performance of decoder was dependent not only on the classification accuracy of encoder but also on its prediction error (variance from 1 or 101).

In experiment two, the encoder rats did not use the discrimination bars for tactile discrimination but received 101 or 1 DCS pulses respectively for virtual narrow and virtual wide trials, and the neuronal response from the end of stimulation was sent to the decoding algorithm to transform into no. of pulses to be delivered to the decoder.

4.3.2 Surgery for implantation of DCS electrode and microelectrode array

Custom build movable microelectrode bundles or fixed arrays were implanted in the M1, S1 and striatal areas of rats (see Fig 3.4 in chapter 3). The stereotaxic coordinates for each of the areas relative to bregma in mm are: M1 [AP: 0 mm; ML: 1.6 mm; DV: -1

mm], S1 [AP: -3 mm; ML: 5.5 mm; DV: -1.25 mm], STR [AP: 0 mm; ML: 3.5 mm; DV: -4.5 mm]. Rats that were trained on the aperture width discrimination task and used as 'encoders' for brainet experiment one (n=4) were implanted bilaterally in M1 and STR, but unilaterally in the left S1 hemisphere. Out of 10 rats that were used as 'decoders' overall, (n=3) were used as encoders in experiment two, out of which, 2 of them had unilateral M1, S1 and STR electrodes in left hemisphere, while, 1 rat had unilateral M1 and S1 electrode in left hemisphere. Bipolar dorsal column electrodes were implanted in the epidural space between T2 vertebra and spinal cord as explained in previous chapter (see methods, chapter 2)

4.3.3 Neurophysiological Recording and Dorsal Column Stimulation

Neuronal data was sampled from the recording electrodes at 40 KHz using a Multichannel Acquisition Processor (Plexon Inc., Dallas, TX). Single and multi-units were sorted online using (SortClient 2002, Plexon Inc., Dallas, TX) and interfaced with Matlab (8.4.0, Mathworks, Natick, MA) for real-time analysis and classification.

DCS consisted of charge balanced biphasic square pulses (between 1 and 100 in number) of 200 μsec duration delivered at 100 Hz. Stimulation intensities were determined during each session and set at a value between sensory and discomfort threshold (therapeutic range with intensities that varied from 110 μA to 600 μA).

4.4.4 Neural Decoding Algorithm

The same approach as described in (Chapter 3, section 3.3.6) was used to create a logistic regression learning algorithm for classification of encoder trials. Single and multi-unit activity was sampled for 1 sec starting from the time the encoder rat crossed the photobeam in the discrimination bars for experiment one and for 500 msec starting from the time stimulation ended (to avoid effect of stimulation artifact) for encoder rat in experiment two. Spiking data was binned in 250 msec and 100 msec bins respectively for experiment one and two. The decoding algorithm calculated the number of DCS pulses (between 1 and 101) to be delivered to the decoder rats.

4.4.5 Data Analysis

Percentage correct trials was used to assess behavioral performance of all rats. Performance of decoding algorithm was measured by calculating the percentage of trials correctly predicted from entire session. Prediction error was calculated as mean squared error of expected value from predicted value using all trials from the session. Comparison of different groups or conditions was performed using (one way ANOVA), followed by post-hoc comparison tests. Whenever distributions failed the normality test, non-parametric tests such as Mann-Whitney or Kruskal-Wallis were used. Spearman's Rank Correlation test was used to measure if correlation were significant.

4.4 Results

4.4.1 A brainet for cortico-spinal communication of real and artificial tactile information

Rats that were previously trained to discriminate the aperture width using their whiskers (encoder) and to discriminate between 101 and 1 DCS pulses (decoders) were used in the two 'brainet' experiments.

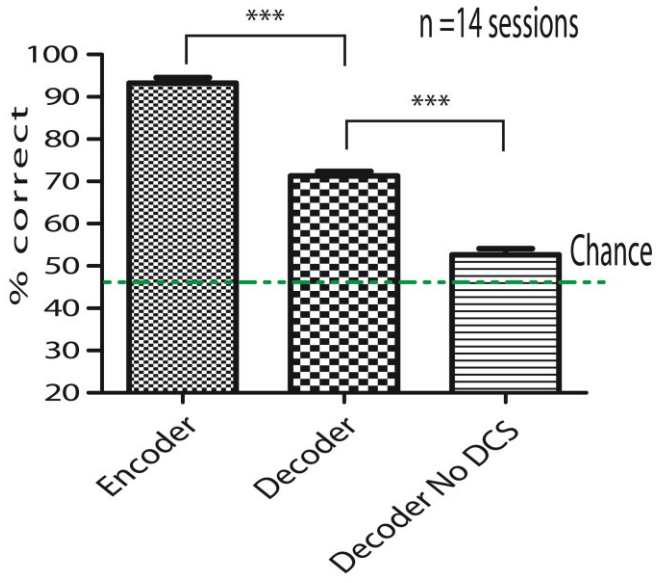

Figure 4.2 Performance of encoder and decoder during transfer of tactile information through a cortico-spinal brainet. Decoder rats performed significantly above chance levels during the real-time transfer of tactile information. There was significant difference in decoder performance when stimulation amplifiers were switched off.

For the first experiment, encoder rats were trained to discriminate between 'narrow' and 'wide' aperture widths using their large vibrissae in the aperture width tactile discrimination behavioral setup. Single and multi-unit data from a total of 798 units sampled from encoders (n=4) was transformed into DCS patterns (between 1 and 101 pulses) using a decoding algorithm (check methods) and sent to the spinal cord of decoder rats, n=6 (from those trained to discriminate between 101 vs 1 DCS pulses, shown in fig

4.1) thus creating a real-time cortico-spinal interface. Instead of using binary classification the no. of pulses delivered to the decoder took any value between 1 and 101 thus forcing the decoder to constantly change its discrimination threshold. The encoder rats performed better (93.21 ± 1.33 % correct trials, Fig 4.2) than the decoder rats (71.33 ± 1.04 % correct trials, Fig 4.2) during the interface (n=14 sessions with 71.50 ± 4.48 trials). Although the performance of decoders was lower than encoders, it was considerably above chance levels (Binomial test: $P<0.001$ in all sessions), with the best performance of 82% in 100 trials. The performance of decoders fell to chance levels (52.63 ± 1.48 % correct trials, fig 4.2) when the stimulation amplifiers were turned off.

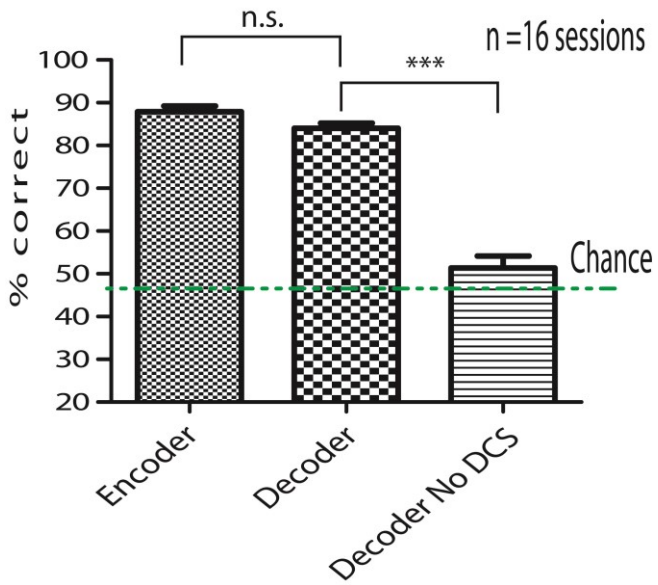

Figure 4.3 Performance of encoder and decoder during transfer of artificial tactile information through a cortico-spinal brainet. Decoder rats performed significantly above chance levels but not significantly different than the encoders. There was significant difference in decoder performance when stimulation amplifiers were switched off.

In the second experiment, we used pairs of rats only from the DCS group who had learnt to successfully discriminate between 101 and 1 DCS pulses for the cortico-spinal interface. Rats that had previously implanted multielectrode arrays served as encoders. The encoder (n=3) rats received DCS with 51 pulses for the 'virtual narrow' trial and 1 pulse for 'virtual wide'. Single and multi-unit activity from 1022 units was sampled for 500 msec from the time the stimulation ended and sent to the decoding algorithm to calculate the no. of pulses (between 101 and 1) to be delivered to spinal cord of decoder (n=6) rats. The nature of the cortico-spinal interface was similar to experiment one except that decoding was performed on the neuronal response to artificial tactile information delivered by DCS instead of the real tactile information acquired by whiskers. Encoder rats performed slightly better (87.88 ± 1.34 % correct trials, Fig 4.3) than decoders (84.03 ± 1.21 % correct trials, Fig 4.3) during the cortico-spinal interface (n=16 sessions with 97.75 ± 2.82 trials). As expected, the performance of decoders was considerably above chance levels (Binomial test: $P<0.001$ in all sessions), with best performance of 92.22% in 90 trials. Like experiment one, the performance of decoders fell to chance levels (51.37 ± 2.79 % correct trials, fig 4.3) when the stimulation amplifier used for decoders was switched off.

4.4.2 Dynamic nature of the cortico-spinal brainet

Performance of decoders depended on how precisely the neuronal activity of encoders was decoded measured as prediction error (explained in methods). Fig 4.4 shows that, although, the performance of decoders fluctuated in the initial trials it stabilized

gradually as the session progressed suggesting that both the neuronal signals of encoders and discrimination threshold of decoders reached a steady state.

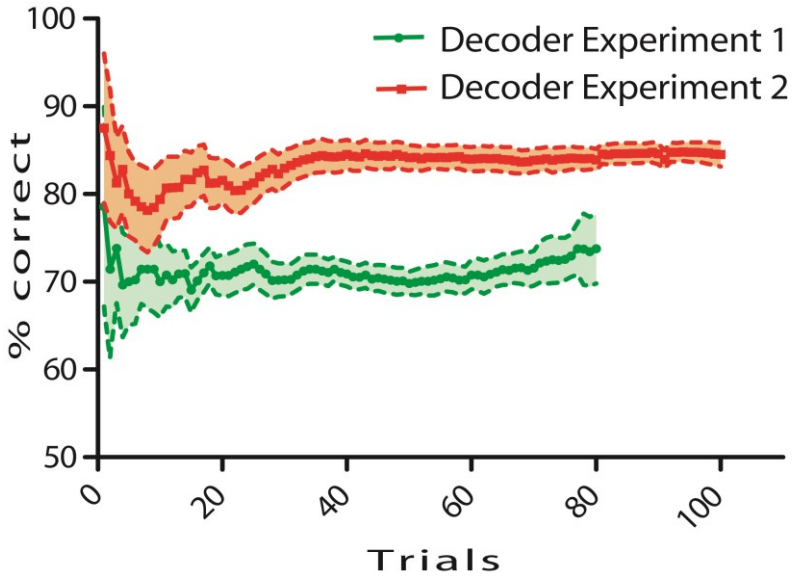

Figure 4.4 Progression of decoder performance for experiment 1 and 2. Decoder rats during the transfer of artificial tactile information (experiment 2) performed consistently better throughout the session as compared to decoders during the transfer of whisker tactile information (experiment 1)

However, the overall performance of decoders in experiment two (red trace) was always higher than those in experiment one (green trace). Because the performance of decoders depended not only on the decoding accuracy of encoder signals but also on the variance of predicted value from the expected value (calculated as prediction error), there was significant negative correlation (Spearman test: $r=0.8589$, $p<0.0001$) between the decoder performance and the prediction error during the interface (Fig 4.5).

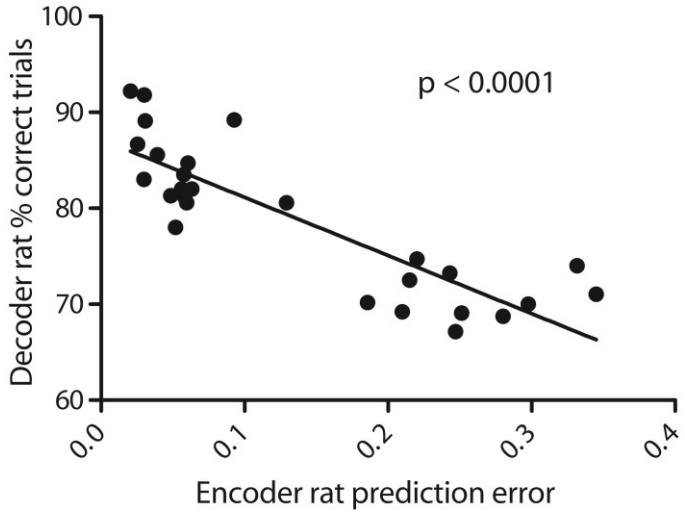

Figure 4.5 Correlation between decoder rats performance and encoder rats prediction error. There was significant negative correlation between the performance of decoders (including both experiments: whisker tactile and artificial tactile cortico-spinal brainet) and the prediction error of encoders.

4.4.3 Real and artificial tactile encoding in multiple cortico-striatal areas

Next we studied the encoding of tactile information in various cortical and sub-cortical regions from experiment one. We noticed that there was significant tactile processing not only in M1 and S1 as reported before but also in the striatum (Fig 4.6). We processed the encoders neuronal data through our decoding algorithm, first, using individual areas, then pairs of areas, followed by all areas together, to obtain the decoding performance for the entire session of the cortico-spinal interface and found that (Fig 4.7a) S1 had the best average encoding (63.66%) followed by striatum (60.12%) and then by M1 (57.78%). The decoding performance improved when pairs of two areas were used together: S1,M1 (66.17%), M1,STR (67.04%) and S1,STR (70.16%). When all three areas were used, maximum average decoding performance (72.25%) was obtained.

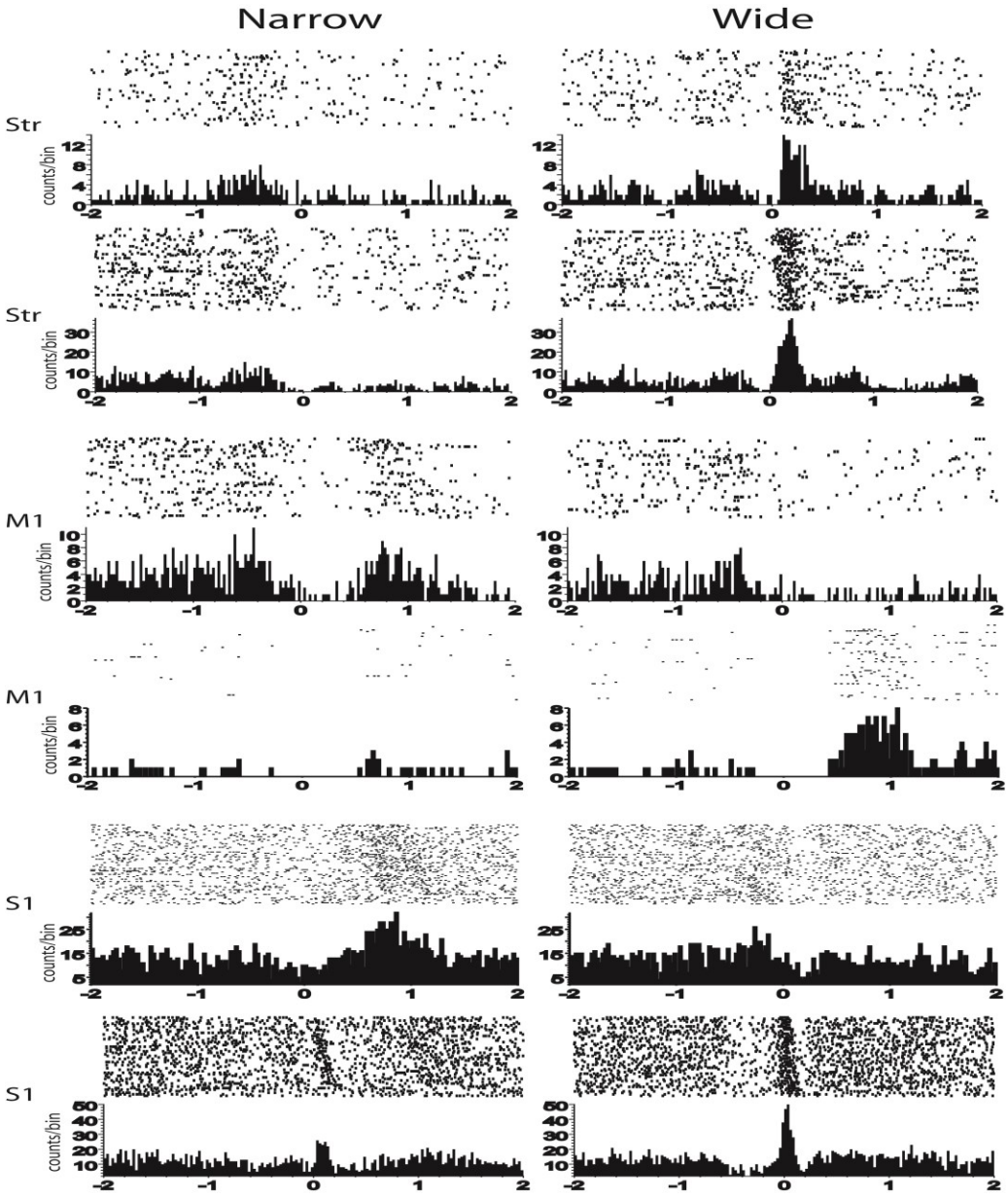

Figure 4.6 Peri Stimulus Time Histogram of M1, S1 and STR neurons. Time t=0, corresponds to encoder rat crossing the discrimination bars. Left column represents neuronal modulation during a 'narrow' trials while right column represents same neurons during wide trials.

This suggests that tactile information is distributed in multiple cortical and subcortical areas. Also, there was a clear linear relation between the number of areas used for decoding and decoding performance.

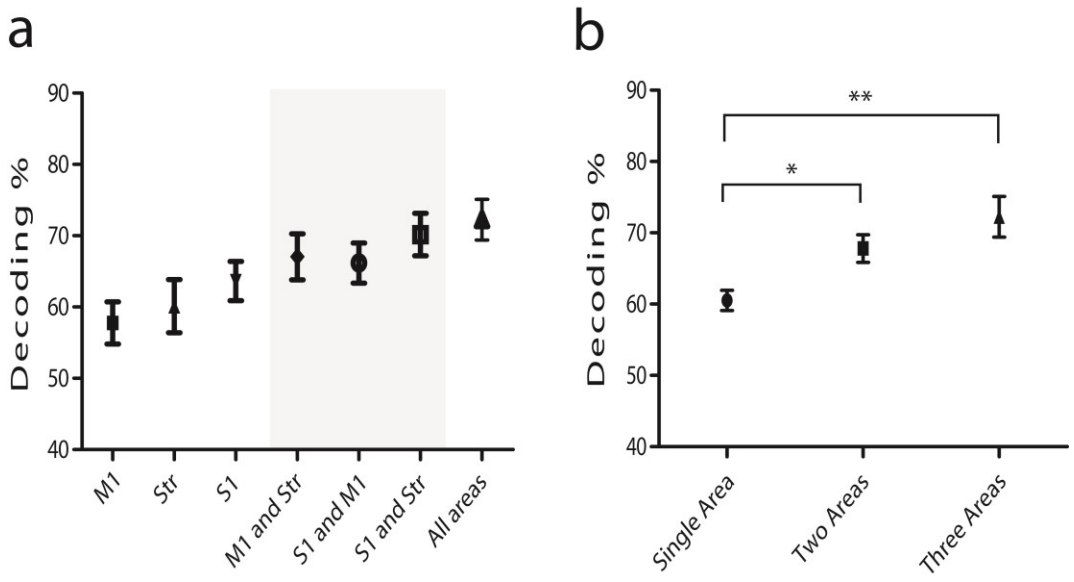

Figure 4.7 Decoding performance of classifier based on encoder neuronal signals in experiment one. a) Individual areas and combination of areas show difference in decoding performance. b) Decoding performance of classifier improves significantly when multiple areas are used for decoding.

Decoding when averaged for all single area [60.52 ± 1.42] values across all sessions was significantly lower than that averaged for two areas [67.79 ± 1.92] ($p<0.05$, Newman-Keuls Multiple Comparison test after 1 way ANOVA) or three areas [72.25 ± 2.84] ($p<0.01$, Newman-Keuls Multiple Comparison test after 1 way ANOVA) taken together (Fig 4.7b). Although, evidence of tactile encoding in striatum has not been reported before, our best decoding performance using only striatal units was 84.47%, suggesting that striatum plays an integral role in processing of tactile information.

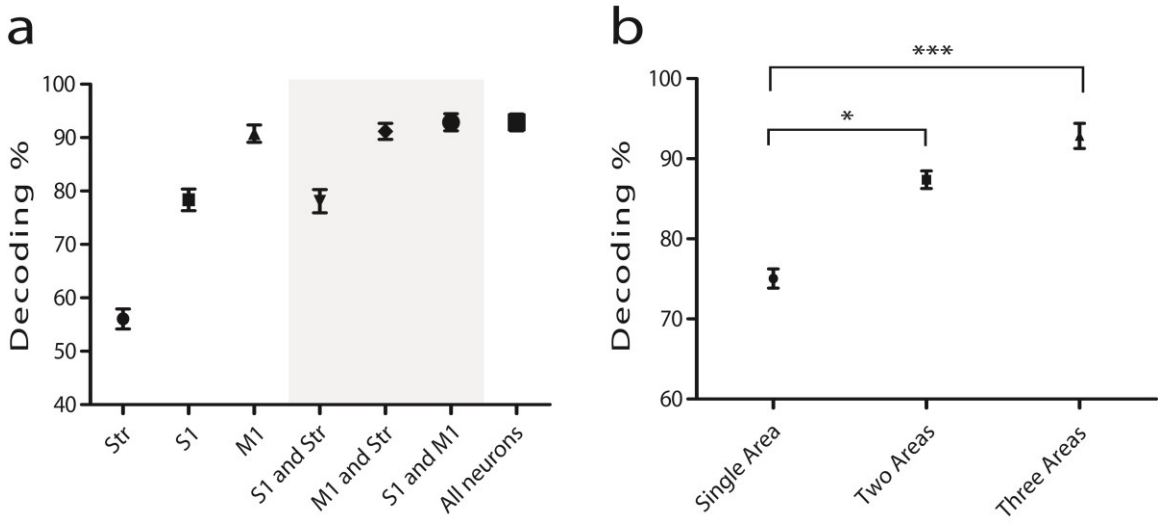

Figure 4.8 Decoding performance of classifier based on encoder neuronal signals in experiment two. a) Individual areas and combination of areas show difference in decoding performance. b) Decoding performance of classifier improves significantly when multiple areas are used for decoding

Similarly, we analyzed how DCS induced tactile sensations were encoded in multiple brain areas in the encoders of experiment two by passing the neuronal data through our decoding algorithm and found that (Fig 4.8a) striatal units alone resulted in a mean decoding performance of (56.05%), while S1 and M1 alone resulted in (78.35%) and (90.77%) respectively. On pairing areas together mean decoding increased to, 78.1 % for S1, STR; 91.17% for M1, STR and 92.88% for S1, M1.

Average decoding when all M1, S1 and STR were taken together was 92.86%. Also, decoding when averaged for all single area [75.06 ±1.19] values across all sessions was significantly lower than that averaged for two areas [87.38 ± 1.1] ($p<0.05$, Dunn's Multiple Comparison test after Kruskal-Wallis) or three areas [92.86 ± 1.56] ($p<0.01$,

Dunn's Multiple Comparison test after Kruskal-Wallis) taken together (Fig 4.8b). This suggests that DCS induced artificial sensations are encoded in multiple cortico-striatal areas and can be successfully decoded for further transfer or processing.

4.5 Discussion

We were able to develop a cortico-spinal brainet transferring real as well as artificial tactile information between two rats demonstrating the first of its kind neural interface where spinal cord was used as a channel for both encoding and decoding of tactile data. We showed that both real and artificial tactile information is encoded in multiple corticostriatal areas and demonstrated that it could be successfully decoded by employing decoding strategies that employ multiple areas in the brain.

In our experiments, we obtained a higher mean performance of decoders (71.33 ± 1.04 %) during the cortico-spinal interface as compared to an earlier study (Pais-Vieira *et al.*, 2013a) where tactile information was transmitted to decoder rats using ICMS of S1 (62.34 ± 0.59 %). The decoders in that study reached a maximum mean performance of (78.77 ± 2.1 %) during initial training which was considerably lower than what was achieved by using DCS to train our rats (91.75 ± 1.36 %). This indicates that animals can discriminate tactile information better when sent through the dorsal columns of spinal cord instead of directly in the somatosensory cortex or suggests that the dorsal column medial lemniscal pathway could be a better filter for processing tactile information as it travels along its way to the cortex.

Additionally, the performance of our decoders in experiment two was consistently higher than those in experiment one. We observed that, on using DCS to encode artificial tactile information in encoders, and subsequently using the neuronal modulations for decoding of their response, the prediction error was reduced, which resulted in better decoding accuracy, reflected by higher performance of decoders. This suggests that DCS can be used as a substitute for ICMS for providing binary cues to a brainet of multiple connected brains in order to perform linear, sequential and parallel computations (Pais-Vieira *et al.*, 2015).

We have shown earlier that tactile processing takes place in multiple thalamo-cortical areas (Krupa *et al.*, 2004; Pantoja *et al.*, 2007; Wiest *et al.*, 2010; Pais-Vieira *et al.*, 2013b) and also in the basal forebrain area (Thomson *et al.*, 2014). It is also known that striatum plays an important role in learning of motor tasks (Thorn *et al.*, 2010; Koralek *et al.*, 2012), but our results indicate that striatum also plays a crucial role in tactile processing. A recent study using DCS for alleviating Parkinson's disease symptoms in marmoset monkeys shows that DCS modulates neuronal activity in various cortical, thalamic and striatal structures (Santana *et al.*, 2014). Thus, our finding that artificial tactile information delivered through DCS was encoded in M1, S1 and striatum suggests that DCS activation of afferent dorsal column fibers distributes artificial tactile information throughout the brain, thereby making DCS an efficient channel for BMI applications that need a feedback pathway to the brain.

Our experiments demonstrate a proof of concept for a Cortico-spinal patient-therapist interface where neuronal activity of a patient can be directly modulated by the

therapist using their brain signals. Recent demonstration of brainets where multiple animal brains worked together to fulfill a common task (Pais-Vieira *et al.*, 2015; Ramakrishnan *et al.*, 2015) suggest that such brainets can be used for testing complex social behaviors and understand how different organisms communicate with each other or modulate each other's behaviors. Although, in the current study we weren't able to record the neuronal activity of decoders as they adapted their behaviors based on signals from the encoders, future work will focus on using brainets, to understand how complex adaptations emerge between different organisms or for studying the dynamic changes in a diseased brain, when introduced in a brainet involving healthy brains, for the treatment of neurological disorders.

5. Conclusion

5.1 Summary of Contributions and Unresolved Questions

In this dissertation, I have demonstrated the use of electrical stimulation of the dorsal columns of the spinal cord, a semi-invasive procedure, referred to as Dorsal Column Stimulation (DCS) as an effective technique to transmit both therapeutic as well as somatosensory information to the brain. Spinal cord stimulation has been used for decades for the treatment of chronic pain, but it has never been explored as a technique to disrupt ongoing pathological activity in supraspinal structures or to train animals in goal-directed behavioral tasks. The goal of this dissertation was to explore these questions.

To test the long term benefits of DCS, I used the 6-OHDA rat model of Parkinson's disease. I found that continuous 30 minutes of stimulation twice a week, resulted in a dramatic recovery of weight loss and motor deficits associated with this model. Surprisingly, the recovery of motor symptoms was paralleled by protection of the dopaminergic neurons from the SNc. Recent work in mice and marmoset monkeys has demonstrated that the acute effect of DCS on PD symptoms is facilitated by corticostriatal desynchronization (Fuentes *et al.*, 2009; Santana *et al.*, 2014). However, it is not yet understood how DCS has a long term neuroprotective effect. Following the publication of our study, another group replicated the neuroprotective effect of DCS using the same 6-OHDA model (Shinko *et al.*, 2014). They found that, 1 hour of DCS for 16 consecutive days resulted in improvement of PD symptoms and significant preservation of tyrosine

hydroxylase (TH) fibers in the striatum and TH-positive neurons in the SNc. They also found that DCS treatment upregulated the levels of vascular endothelial growth factor and suggest that this could be partially responsible for the DCS neuroprotective effect.

Future studies employing closed loop DCS or continuous DCS throughout the course of the experiment could be useful to study if the neuroprotective effect can be enhanced by increasing the amount of stimulation provided. So far, there have been numerous clinical studies in PD patients showing that DCS alleviates PD symptoms of tremor, rigidity and improves gait and posture (Agari & Date, 2012; Fenelon *et al.*, 2012; Landi *et al.*, 2012; Hassan *et al.*, 2013b; Arii *et al.*, 2014). Due to the highly invasive nature of DBS, it is likely that DCS would emerge as an alternative for the treatment of Parkinson's Disease.

Subsequently, I investigated the ability of animals to discriminate multiple artificial tactile sensations generated by varying temporal patterns of DCS. Rats were able to successfully discriminate up to four different artificial percepts generated by DCS. Previous studies using ICMS as an artificial tactile channel to the brain in monkeys, have been limited to 3 discriminable percepts (O'Doherty *et al.*, 2011). Thus, my demonstration that, rats learnt to differentiate 4 tactile patterns is a highly significant finding, which, opens up new questions regarding the role of spinal cord in sensory perception. Although it is not known if DCS activates tactile or proprioceptive pathways, based on my observation, I hypothesize that it could be used for encoding of both. Future studies employing DCS for sensory feedback in a BMI application could attempt to resolve this question.

Finally, to solidify my claim that DCS can be used to communicate relevant information with the brain, I developed a real-time cortico-spinal interface for the transfer of real as well as artificial tactile information between two animals. DCS was used to encode information in an encoder rat, which was decoded in real time using a neural decoding algorithm, and transformed into number of pulses to be delivered to the decoder rat's spinal cord. This resulted in a complex brainet that was dependent on the prediction accuracy of one rat's neuronal data and the discrimination threshold of another. Recently, a similar interface showed the transfer of cortical signals from one monkey to the spinal cord of another paralyzed monkey (Shanechi *et al.*, 2014), however, in that case DCS was used to control efferent limb movement and not for afferent communication. Future experiments can be conducted to create a cortico-spinal brainet between a healthy brain and a disordered brain to investigate if such an interface can facilitate neuroplasticity required for faster recovery.

5.2 Future Directions

5.2.1 Closed loop DCS triggered by motor initiation or cortico-striatal synchronization

In the experiments described in chapter 2, dorsal column stimulation was manually triggered at the start of the session and stopped after a fixed time interval. Recent studies involving DBS have tried to incorporate a closed loop feedback mechanism for the delivery of deep brain stimulation pulses. It was shown that closed loop DBS paradigms involving stimulation of GPi triggered by M1 neuronal activity had a greater effect on akinesia and cortical or pallidal discharge patterns as compared to open loop DBS paradigms in MPTP

treated monkeys (Rosin *et al.*, 2011). It was also observed that closed loop DBS reduced the stimulation frequency and increased the variability of interstimulus interval, but further analysis revealed that it wasn't the change in statistics of stimulation pattern, but rather the fact that stimulation pattern reflected ongoing M1 activity that promoted behavioral improvements, thereby highlighting the efficacy of the closed loop paradigm. A similar approach could be used for developing a closed loop DCS paradigm where M1 or striatal neuronal activity can be used to trigger trains of DCS pulses. One approach would be to use characteristic PD low frequency oscillatory activity in cortico-striatal neurons as a trigger or, DCS triggered by cortico-striatal synchronization of local field potentials (LFP). Another approach would be to detect neuronal patterns of locomotion initiation and trigger stimulation at the onset of locomotion epochs to facilitate movement. Preliminary results from control animals indicate that, there is a clear modulation of LFP low frequency power at the onset of locomotion which could be used to initiate DCS in PD rats. This approach could eventually be translated in PD patients wherein therapeutic DCS would be initiated only when the patients intend to move and would switch off at other times.

5.2.2 DCS for somatosensory feedback in BMIs

In chapter 3, I've shown that rats can successfully discriminate four different stimulation patterns delivered through DCS. Although it is not known how tactile percepts were generated that lead to conscious discrimination ability in rats, it would be imperative to incorporate DCS as a feedback channel in a Brain Machine Interface experiment. (O'Doherty *et al.*, 2011) have created a Brain Machine Brain Interface where monkeys

operated a virtual arm using a BMI driven by cortical motor signals, while, ICMS was used to provide feedback about active touch as the animal moved its arm across 3 different virtual textures. Given the knowledge that rats were able to discriminate 4 tactile sensations generated by DCS, a similar experiment using DCS in monkeys could be performed where, DCS could either encode information about virtual tactile surfaces or provide proprioceptive feedback about the monkey's limb position in space.

5.2.3 Spatio-temporal patterns for artificial tactile sensation and computational modelling of DCS

In chapter 3, different temporal patterns of DCS were used to train rats to discriminate 4 artificial tactile sensation in order to obtain a water reward using bipolar stimulation electrodes placed transversely on the epidural surface. It is not yet known if DCS encodes artificial tactile information or proprioceptive information. However, it will be interesting to create additional stimulation channels along the dorsal spinal surface to generate spatio-temporal patterns of DCS

It is known that the dorsal column medial lemniscal pathway crosses over to the contralateral side and innervates contralateral somatosensory areas. It could be possible to utilize the somatotopy of this pathway and generate artificial sensations in the contralateral cortex in order to cue the rats in a particular direction. Such an approach has been demonstrated in an unpublished study from our group where, somatotopically organized spatio-temporal patterns of ICMS increased the rate of learning in rats that responded to infrared light.

To aid our understanding of how DCS creates tactile sensations or paresthesia in various dermatomes, it will be useful to create computational models of the spinal cord to study the current and charge distributions along the dorsal surface created by various spatio-temporal patterns of DCS.

5.2.4 Cortico-spinal brainet for Parkinson's Disease

In Chapter 4, I have created the first of its kind neural interface for cortico-spinal communication. My intention was to demonstrate a proof of concept that, cortico-spinal communication between two rats could be possible and later use it to treat Parkinson's Disease. Parkinsonian animals have trouble initiating movement and their neuronal activity is dominated by low frequency oscillations (Bergman *et al.*, 1994). Previously, it has been shown that DCS alleviates Parkinsonian symptoms by desynchronizing these oscillations (Fuentes *et al.*, 2009; Santana *et al.*, 2014). Although, closed loop stimulation will enable DCS to be controlled by the animal's cortical activity, an experiment where a healthy animal uses its neuronal activity to trigger DCS in a Parkinsonian animal would be the optimum application of my cortico-spinal brainet. Such a demonstration could be the basis of a future patient-therapist interface where, a healthy brain is able to modulate the neuronal activity of a disordered brain in order to facilitate neuroplasticity, learning and rehabilitation.

5.2.5 DCS for treatment of other neurological disorders

In chapter 2, I have demonstrated that DCS has a neuroprotective effect on the dopaminergic neurons associated with Parkinson's Disease. Other reports from our group have shown that the therapeutic effect of DCS is facilitated by DCS induced modulation

of neuronal activity in supraspinal structures (Fuentes *et al.*, 2009; Santana *et al.*, 2014). It is also known that electrical stimulation of the trigeminal nerve is effective in desynchronizing the neuronal coherence observed during epileptic seizures in awake rats, resulting in reduction of seizure activity (Fanselow *et al.*, 2000). Using similar approach as that used for treating Parkinson's Disease, closed loop DCS could be used to detect seizure activity in an animal model of epilepsy and trigger a train of pulses, in order to desynchronize cortical activity associated with epilepsy.

Cortical activity of autistic patients is characterized by an increase in localized cortical connectivity (Rinaldi *et al.*, 2008; Qiu *et al.*, 2011). This localized hyperconnectivity is hypothesized to be responsible for the pathological synchronization and seizure like activity in cortical areas of autistic patients. Since, we have established that, DCS can be used as a therapeutic intervention to cause corticostriatal desynchronization, it would be important to test the efficacy of DCS in an animal model of autism and assess if it can reduce the epileptiform activity associated with it. Additionally, a brain to brain interface approach can be used with autistic individuals with sensory deficits, whereby, sensory cues during social interactions can be translated from healthy individual into electrical stimulation of the deficient sensory modality of an autistic patient.

6. Bibliography

Abercrombie, M. (1946) Estimation of nuclear population from microtome sections. *The Anatomical record*, **94**, 239-247.

Agari, T. & Date, I. (2012) Spinal cord stimulation for the treatment of abnormal posture and gait disorder in patients with Parkinson's disease. *Neurologia medico-chirurgica*, **52**, 470-474.

Aguilar, J., Pulecchi, F., Dilena, R., Oliviero, A., Priori, A. & Foffani, G. (2011) Spinal direct current stimulation modulates the activity of gracile nucleus and primary somatosensory cortex in anaesthetized rats. *J Physiol*, **589**, 4981-4996.

Arii, Y., Sawada, Y., Kawamura, K., Miyake, S., Taichi, Y., Izumi, Y., Kuroda, Y., Inui, T., Kaji, R. & Mitsui, T. (2014) Immediate effect of spinal magnetic stimulation on camptocormia in Parkinson's disease. *Journal of neurology, neurosurgery, and psychiatry*, **85**, 1221-1226.

Bachmann, C.G. & Trenkwalder, C. (2006) Body weight in patients with Parkinson's disease. *Mov Disord*, **21**, 1824-1830.

Benabid, A.L. (2003) Deep brain stimulation for Parkinson's disease. *Curr Opin Neurobiol*, **13**, 696-706.

Bergman, H., Wichmann, T., Karmon, B. & DeLong, M.R. (1994) The primate subthalamic nucleus. II. Neuronal activity in the MPTP model of parkinsonism. *Journal of neurophysiology*, **72**, 507-520.

Blandini, F., Levandis, G., Bazzini, E., Nappi, G. & Armentero, M.T. (2007) Time-course of nigrostriatal damage, basal ganglia metabolic changes and behavioural alterations following intrastriatal injection of 6-hydroxydopamine in the rat: new clues from an old model. *The European journal of neuroscience*, **25**, 397-405.

Brown, P. (2003) Oscillatory nature of human basal ganglia activity: relationship to the pathophysiology of Parkinson's disease. *Mov Disord*, **18**, 357-363.

Burns, R.S., Chiueh, C.C., Markey, S.P., Ebert, M.H., Jacobowitz, D.M. & Kopin, I.J. (1983) A primate model of parkinsonism: selective destruction of dopaminergic neurons in the pars compacta of the substantia nigra by N-methyl-4-phenyl-1,2,3,6-tetrahydropyridine. *Proceedings of the National Academy of Sciences of the United States of America*, **80**, 4546-4550.

Carlsson, A. (1972) Biochemical and pharmacological aspects of Parkinsonism. *Acta neurologica Scandinavica. Supplementum*, **51**, 11-42.

Carmena, J.M., Lebedev, M.A., Crist, R.E., O'Doherty, J.E., Santucci, D.M., Dimitrov, D.F., Patil, P.G., Henriquez, C.S. & Nicolelis, M.A. (2003) Learning to control a brain-machine interface for reaching and grasping by primates. *PLoS biology*, **1**, E42.

Cenci, M.A., Whishaw, I.Q. & Schallert, T. (2002) Animal models of neurological deficits: how relevant is the rat? *Nat Rev Neurosci*, **3**, 574-579.

Chapin, J.K., Moxon, K.A., Markowitz, R.S. & Nicolelis, M.A. (1999) Real-time control of a robot arm using simultaneously recorded neurons in the motor cortex. *Nature neuroscience*, **2**, 664-670.

Chen, H., Zhang, S.M., Hernan, M.A., Willett, W.C. & Ascherio, A. (2003) Weight loss in Parkinson's disease. *Annals of neurology*, **53**, 676-679.

Cicchetti, F., Brownell, A.L., Williams, K., Chen, Y.I., Livni, E. & Isacson, O. (2002) Neuroinflammation of the nigrostriatal pathway during progressive 6-OHDA dopamine degeneration in rats monitored by immunohistochemistry and PET imaging. *The European journal of neuroscience*, **15**, 991-998.

Compton, A.K., Shah, B. & Hayek, S.M. (2012) Spinal cord stimulation: a review. *Curr Pain Headache Rep*, **16**, 35-42.

Costa, R.M., Lin, S.C., Sotnikova, T.D., Cyr, M., Gainetdinov, R.R., Caron, M.G. & Nicolelis, M.A. (2006) Rapid alterations in corticostriatal ensemble coordination during acute dopamine-dependent motor dysfunction. *Neuron*, **52**, 359-369.

D'Mello, R. & Dickenson, A.H. (2008) Spinal cord mechanisms of pain. *Br J Anaesth*, **101**, 8-16.

Dawson, T.M. & Dawson, V.L. (2002) Neuroprotective and neurorestorative strategies for Parkinson's disease. *Nature neuroscience*, **5 Suppl**, 1058-1061.

Dejongste, M.J., Hautvast, R.W., Ruiters, M.H. & Ter Horst, G.J. (1998) Spinal Cord Stimulation and the Induction of c-fos and Heat Shock Protein 72 in the Central Nervous System of Rats. *Neuromodulation : journal of the International Neuromodulation Society*, **1**, 73-84.

Deumens, R., Blokland, A. & Prickaerts, J. (2002) Modeling Parkinson's disease in rats: an evaluation of 6-OHDA lesions of the nigrostriatal pathway. *Experimental neurology*, **175**, 303-317.

Dimitrijevic, M.R., Faganel, J., Sharkey, P.C. & Sherwood, A.M. (1980) Study of sensation and muscle twitch responses to spinal cord stimulation. *International rehabilitation medicine*, **2**, 76-81.

Ekstrand, M.I., Terzioglu, M., Galter, D., Zhu, S., Hofstetter, C., Lindqvist, E., Thams, S., Bergstrand, A., Hansson, F.S., Trifunovic, A., Hoffer, B., Cullheim, S., Mohammed, A.H., Olson, L. & Larsson, N.G. (2007) Progressive parkinsonism in mice with respiratory-chain-deficient dopamine neurons. *Proceedings of the National Academy of Sciences of the United States of America*, **104**, 1325-1330.

Fahn, S. (2003) Description of Parkinson's disease as a clinical syndrome. *Ann N Y Acad Sci*, **991**, 1-14.

Fanselow, E.E., Reid, A.P. & Nicolelis, M.A. (2000) Reduction of pentylenetetrazole-induced seizure activity in awake rats by seizure-triggered trigeminal nerve stimulation. *The Journal of neuroscience : the official journal of the Society for Neuroscience*, **20**, 8160-8168.

Fenelon, G., Goujon, C., Gurruchaga, J.M., Cesaro, P., Jarraya, B., Palfi, S. & Lefaucheur, J.P. (2012) Spinal cord stimulation for chronic pain improved motor function in a patient with Parkinson's disease. *Parkinsonism & related disorders*, **18**, 213-214.

Ferro, M.M., Bellissimo, M.I., Anselmo-Franci, J.A., Angellucci, M.E., Canteras, N.S. & Da Cunha, C. (2005) Comparison of bilaterally 6-OHDA- and MPTP-lesioned rats as models of the early phase of Parkinson's disease: histological, neurochemical, motor and memory alterations. *J Neurosci Methods*, **148**, 78-87.

Fitzsimmons, N.A., Drake, W., Hanson, T.L., Lebedev, M.A. & Nicolelis, M.A. (2007) Primate reaching cued by multichannel spatiotemporal cortical microstimulation. *The Journal of neuroscience : the official journal of the Society for Neuroscience*, **27**, 5593-5602.

Freire, M.A., Oliveira, R.B., Picanco-Diniz, C.W. & Pereira, A., Jr. (2007) Differential effects of methylmercury intoxication in the rat's barrel field as evidenced by NADPH diaphorase histochemistry. *Neurotoxicology*, **28**, 175-181.

Fuentes, R., Petersson, P. & Nicolelis, M.A. (2010) Restoration of locomotive function in Parkinson's disease by spinal cord stimulation: mechanistic approach. *The European journal of neuroscience*, **32**, 1100-1108.

Fuentes, R., Petersson, P., Siesser, W.B., Caron, M.G. & Nicolelis, M.A. (2009) Spinal cord stimulation restores locomotion in animal models of Parkinson's disease. *Science*, **323**, 1578-1582.

Gaunt, R.A., Prochazka, A., Mushahwar, V.K., Guevremont, L. & Ellaway, P.H. (2006) Intraspinal microstimulation excites multisegmental sensory afferents at lower stimulus levels than local alpha-motoneuron responses. *Journal of neurophysiology*, **96**, 2995-3005.

Gironell, A., Pascual-Sedano, B., Otermin, P. & Kulisevsky, J. (2002) [Weight gain after functional surgery for Parkinsons disease]. *Neurologia*, **17**, 310-316.

Gradinaru, V., Mogri, M., Thompson, K.R., Henderson, J.M. & Deisseroth, K. (2009) Optical deconstruction of parkinsonian neural circuitry. *Science*, **324**, 354-359.

Grau, C., Ginhoux, R., Riera, A., Nguyen, T.L., Chauvat, H., Berg, M., Amengual, J.L., Pascual-Leone, A. & Ruffini, G. (2014) Conscious brain-to-brain communication in humans using non-invasive technologies. *PloS one*, **9**, e105225.

Haber, S.N. (2003) The primate basal ganglia: parallel and integrative networks. *Journal of chemical neuroanatomy*, **26**, 317-330.

Hassan, S., Amer, S., Alwaki, A. & Elborno, A. (2013a) A patient with Parkinson's disease benefits from spinal cord stimulation. *Journal of clinical neuroscience : official journal of the Neurosurgical Society of Australasia*.

Hassan, S., Amer, S., Alwaki, A. & Elborno, A. (2013b) A patient with Parkinson's disease benefits from spinal cord stimulation. *Journal of clinical neuroscience : official journal of the Neurosurgical Society of Australasia*, **20**, 1155-1156.

Heming, E., Sanden, A. & Kiss, Z.H. (2010) Designing a somatosensory neural prosthesis: percepts evoked by different patterns of thalamic stimulation. *Journal of neural engineering*, **7**, 064001.

Hilker, R., Portman, A.T., Voges, J., Staal, M.J., Burghaus, L., van Laar, T., Koulousakis, A., Maguire, R.P., Pruim, J., de Jong, B.M., Herholz, K., Sturm, V., Heiss, W.D. & Leenders, K.L. (2005) Disease progression continues in patients with advanced Parkinson's disease and effective subthalamic nucleus stimulation. *Journal of neurology, neurosurgery, and psychiatry*, **76**, 1217-1221.

Holsheimer, J. (2002) Which Neuronal Elements are Activated Directly by Spinal Cord Stimulation. *Neuromodulation : journal of the International Neuromodulation Society*, **5**, 25-31.

Holsheimer, J. & Barolat, G. (1998) Spinal geometry and paresthesia coverage in spinal cord stimulation. *Neuromodulation : journal of the International Neuromodulation Society*, **1**, 129-136.

Hrdina, P.D. & Dubas, T.C. (1981) Brain distribution and kinetics of desipramine in the rat. *Canadian journal of physiology and pharmacology*, **59**, 163-167.

Kaas, J.H., Qi, H.X., Burish, M.J., Gharbawie, O.A., Onifer, S.M. & Massey, J.M. (2008) Cortical and subcortical plasticity in the brains of humans, primates, and rats after damage to sensory afferents in the dorsal columns of the spinal cord. *Experimental neurology*, **209**, 407-416.

Kirik, D., Rosenblad, C., Burger, C., Lundberg, C., Johansen, T.E., Muzyczka, N., Mandel, R.J. & Bjorklund, A. (2002) Parkinson-like neurodegeneration induced by targeted overexpression of alpha-synuclein in the nigrostriatal system. *The Journal of neuroscience : the official journal of the Society for Neuroscience*, **22**, 2780-2791.

Kish, S.J., Shannak, K. & Hornykiewicz, O. (1988) Uneven pattern of dopamine loss in the striatum of patients with idiopathic Parkinson's disease. Pathophysiologic and clinical implications. *The New England journal of medicine*, **318**, 876-880.

Klein, R.L., Lewis, M.H., Muzyczka, N. & Meyer, E.M. (1999) Prevention of 6-hydroxydopamine-induced rotational behavior by BDNF somatic gene transfer. *Brain Res*, **847**, 314-320.

Knutsson, E. (1972) An analysis of Parkinsonian gait. *Brain*, **95**, 475-486.

Koralek, A.C., Jin, X., Long, J.D., 2nd, Costa, R.M. & Carmena, J.M. (2012) Corticostriatal plasticity is necessary for learning intentional neuroprosthetic skills. *Nature*, **483**, 331-335.

Kordower, J.H. (2000) Neurodegeneration Prevented by Lentiviral Vector Delivery of GDNF in Primate Models of Parkinson's Disease. *Science*, **290**, 767-773.

Krupa, D.J., Wiest, M.C., Shuler, M.G., Laubach, M. & Nicolelis, M.A. (2004) Layer-specific somatosensory cortical activation during active tactile discrimination. *Science*, **304**, 1989-1992.

Landi, A., Trezza, A., Pirillo, D., Vimercati, A., Antonini, A. & Sganzerla, E.P. (2012) Spinal Cord Stimulation for the Treatment of Sensory Symptoms in Advanced Parkinson's Disease. *Neuromodulation : journal of the International Neuromodulation Society*.

Lebedev, M.A. & Nicolelis, M.A. (2006) Brain-machine interfaces: past, present and future. *Trends Neurosci*, **29**, 536-546.

Lenard, L., Karadi, Z., Jando, G., Yoshimatsu, H., Hajnal, A., Sandor, P. & Oomura, Y. (1991) Feeding and body weight regulation after 6-OHDA application into the preoptic area. *Brain Res Bull*, **27**, 359-365.

Linderoth, B. & Foreman, R.D. (1999) Physiology of spinal cord stimulation: Review and update. *Neuromodulation : journal of the International Neuromodulation Society*, **2**, 150-164.

London, B.M., Jordan, L.R., Jackson, C.R. & Miller, L.E. (2008) Electrical stimulation of the proprioceptive cortex (area 3a) used to instruct a behaving monkey. *IEEE Trans Neural Syst Rehabil Eng*, **16**, 32-36.

Macia, F., Perlemoine, C., Coman, I., Guehl, D., Burbaud, P., Cuny, E., Gin, H., Rigalleau, V. & Tison, F. (2004) Parkinson's disease patients with bilateral subthalamic deep brain stimulation gain weight. *Mov Disord*, **19**, 206-212.

Maeda, Y., Ikeuchi, M., Wacnik, P. & Sluka, K.A. (2009) Increased c-fos immunoreactivity in the spinal cord and brain following spinal cord stimulation is frequency-dependent. *Brain Res*, **1259**, 40-50.

Marasco, P.D., Schultz, A.E. & Kuiken, T.A. (2009) Sensory capacity of reinnervated skin after redirection of amputated upper limb nerves to the chest. *Brain*, **132**, 1441-1448.

May, T., Ozden, I., Brush, B., Borton, D., Wagner, F., Agha, N., Sheinberg, D.L. & Nurmikko, A.V. (2014) Detection of optogenetic stimulation in somatosensory cortex by non-human primates--towards artificial tactile sensation. *PloS one*, **9**, e114529.

Melzack, R. & Wall, P.D. (1965) Pain Mechanisms - a New Theory. *Science*, **150**, 971-&.

Mendez, J.S. & Finn, B.W. (1975) Use of 6-hydroxydopamine to create lesions in catecholamine neurons in rats. *Journal of neurosurgery*, **42**, 166-173.

Morgante, L., Morgante, F., Moro, E., Epifanio, A., Girlanda, P., Ragonese, P., Antonini, A., Barone, P., Bonuccelli, U., Contarino, M.F., Capus, L., Ceravolo, M.G., Marconi, R., Ceravolo, R., D'Amelio, M. & Savettieri, G. (2007) How many parkinsonian patients are suitable candidates for deep brain stimulation of subthalamic nucleus? Results of a questionnaire. *Parkinsonism & related disorders*, **13**, 528-531.

Moro, E., Scerrati, M., Romito, L.M., Roselli, R., Tonali, P. & Albanese, A. (1999) Chronic subthalamic nucleus stimulation reduces medication requirements in Parkinson's disease. *Neurology*, **53**, 85-90.

Muller, J., Wenning, G.K., Verny, M., McKee, A., Chaudhuri, K.R., Jellinger, K., Poewe, W. & Litvan, I. (2001) Progression of dysarthria and dysphagia in postmortem-confirmed parkinsonian disorders. *Archives of neurology*, **58**, 259-264.

Nagatsua, T. & Sawadab, M. (2009) L-dopa therapy for Parkinson's disease: past, present, and future. *Parkinsonism & related disorders*, **15 Suppl 1**, S3-8.

Nashold, B.S., Jr., Somjen, G. & Friedman, H. (1972) The effects of stimulating the dorsal columns of man. *Medical progress through technology*, **1**, 89-91.

Nicolelis, M.A., Fuentes, R., Petersson, P., Thevathasan, W. & Brown, P. (2010) Spinal cord stimulation failed to relieve akinesia or restore locomotion in Parkinson disease. *Neurology*, **75**, 1484; author reply 1484-1485.

Nicolelis, M.A. & Lebedev, M.A. (2009) Principles of neural ensemble physiology underlying the operation of brain-machine interfaces. *Nat Rev Neurosci*, **10**, 530-540.

O'Doherty, J.E., Lebedev, M.A., Ifft, P.J., Zhuang, K.Z., Shokur, S., Bleuler, H. & Nicolelis, M.A. (2011) Active tactile exploration using a brain-machine-brain interface. *Nature*, **479**, 228-231.

O'Doherty, J.E., Lebedev, M.A., Li, Z. & Nicolelis, M.A. (2012) Virtual active touch using randomly patterned intracortical microstimulation. *IEEE Trans Neural Syst Rehabil Eng*, **20**, 85-93.

Ondo, W.G., Ben-Aire, L., Jankovic, J., Lai, E., Contant, C. & Grossman, R. (2000) Weight gain following unilateral pallidotomy in Parkinson's disease. *Acta Neurol Scand*, **101**, 79-84.

Pais-Vieira, M., Chiuffa, G., Lebedev, M., Yadav, A. & Nicolelis, M.A. (2015) Building an organic computing device with multiple interconnected brains. *Sci Rep*, **5**, 11869.

Pais-Vieira, M., Lebedev, M., Kunicki, C., Wang, J. & Nicolelis, M.A. (2013a) A brain-to-brain interface for real-time sharing of sensorimotor information. *Sci Rep*, **3**, 1319.

Pais-Vieira, M., Lebedev, M.A., Wiest, M.C. & Nicolelis, M.A. (2013b) Simultaneous top-down modulation of the primary somatosensory cortex and thalamic nuclei during active tactile discrimination. *The Journal of neuroscience : the official journal of the Society for Neuroscience*, **33**, 4076-4093.

Pantoja, J., Ribeiro, S., Wiest, M., Soares, E., Gervasoni, D., Lemos, N.A. & Nicolelis, M.A. (2007) Neuronal activity in the primary somatosensory thalamocortical loop is modulated by reward contingency during tactile discrimination. *The Journal of neuroscience : the official journal of the Society for Neuroscience*, **27**, 10608-10620.

Paxinos, G. & Watson, C. (1997) *The rat brain, in stereotaxic coordinates*. Academic Press, San Diego.

Pirke, K.M., Broocks, A., Wilckens, T., Marquard, R. & Schweiger, U. (1993) Starvation-induced hyperactivity in the rat: the role of endocrine and neurotransmitter changes. *Neurosci Biobehav Rev*, **17**, 287-294.

Pizzolato, G. & Mandat, T. (2012) Deep brain stimulation for movement disorders. *Front Integr Neurosci*, **6**, 2.

Qiu, S., Anderson, C.T., Levitt, P. & Shepherd, G.M. (2011) Circuit-specific intracortical hyperconnectivity in mice with deletion of the autism-associated Met receptor tyrosine kinase. *The Journal of neuroscience : the official journal of the Society for Neuroscience*, **31**, 5855-5864.

Ramakrishnan, A., Ifft, P.J., Pais-Vieira, M., Woo Byun, Y., Zhuang, K.Z., Lebedev, M.A. & Nicolelis, M.A. (2015) Computing Arm Movements with a Monkey Brainet. *Sci Rep*, **5**, 10767.

Rao, R.P., Stocco, A., Bryan, M., Sarma, D., Youngquist, T.M., Wu, J. & Prat, C.S. (2014) A direct brain-to-brain interface in humans. *PloS one*, **9**, e111332.

Rinaldi, T., Silberberg, G. & Markram, H. (2008) Hyperconnectivity of local neocortical microcircuitry induced by prenatal exposure to valproic acid. *Cereb Cortex*, **18**, 763-770.

Roedter, A., Winkler, C., Samii, M., Walter, G.F., Brandis, A. & Nikkhah, G. (2001) Comparison of unilateral and bilateral intrastriatal 6-hydroxydopamine-induced axon terminal lesions: evidence for interhemispheric functional coupling of the two nigrostriatal pathways. *The Journal of comparative neurology*, **432**, 217-229.

Romo, R., Hernandez, A., Zainos, A., Brody, C.D. & Lemus, L. (2000) Sensing without touching: psychophysical performance based on cortical microstimulation. *Neuron*, **26**, 273-278.

Romo, R., Hernandez, A., Zainos, A. & Salinas, E. (1998) Somatosensory discrimination based on cortical microstimulation. *Nature*, **392**, 387-390.

Rosin, B., Slovik, M., Mitelman, R., Rivlin-Etzion, M., Haber, S.N., Israel, Z., Vaadia, E. & Bergman, H. (2011) Closed-loop deep brain stimulation is superior in ameliorating parkinsonism. *Neuron*, **72**, 370-384.

Santana, M.B., Halje, P., Simplicio, H., Richter, U., Freire, M.A., Petersson, P., Fuentes, R. & Nicolelis, M.A. (2014) Spinal cord stimulation alleviates motor deficits in a primate model of Parkinson disease. *Neuron*, **84**, 716-722.

Sauer, H. & Oertel, W.H. (1994) Progressive degeneration of nigrostriatal dopamine neurons following intrastriatal terminal lesions with 6-hydroxydopamine: a combined retrograde tracing and immunocytochemical study in the rat. *Neuroscience*, **59**, 401-415.

Schapira, A.H.V. & Olanow, C.W. (2004) Neuroprotection in Parkinson disease - Mysteries, myths, and misconceptions. *Jama-J Am Med Assoc*, **291**, 358-364.

Schwarting, R.K. & Huston, J.P. (1996) The unilateral 6-hydroxydopamine lesion model in behavioral brain research. Analysis of functional deficits, recovery and treatments. *Prog Neurobiol*, **50**, 275-331.

Shanechi, M.M., Hu, R.C. & Williams, Z.M. (2014) A cortical-spinal prosthesis for targeted limb movement in paralysed primate avatars. *Nature communications*, **5**, 3237.

Shealy, C.N., Mortimer, J.T. & Reswick, J.B. (1967) Electrical inhibition of pain by stimulation of the dorsal columns: preliminary clinical report. *Anesth Analg*, **46**, 489-491.

Shinko, A., Agari, T., Kameda, M., Yasuhara, T., Kondo, A., Tayra, J.T., Sato, K., Sasaki, T., Sasada, S., Takeuchi, H., Wakamori, T., Borlongan, C.V. & Date, I. (2014) Spinal cord stimulation exerts neuroprotective effects against experimental Parkinson's disease. *PloS one*, **9**, e101468.

Shults, C.W., Kimber, T. & Altar, C.A. (1995) BDNF attenuates the effects of intrastriatal injection of 6-hydroxydopamine. *Neuroreport*, **6**, 1109-1112.

Shults, C.W., Kimber, T. & Martin, D. (1996) Intrastriatal injection of GDNF attenuates the effects of 6-hydroxydopamine. *Neuroreport*, **7**, 627-631.

Sotak, B.N., Hnasko, T.S., Robinson, S., Kremer, E.J. & Palmiter, R.D. (2005) Dysregulation of dopamine signaling in the dorsal striatum inhibits feeding. *Brain Res*, **1061**, 88-96.

Spieles-Engemann, A.L., Behbehani, M.M., Collier, T.J., Wohlgenant, S.L., Steece-Collier, K., Paumier, K., Daley, B.F., Gombash, S., Madhavan, L., Mandybur, G.T., Lipton, J.W., Terpstra, B.T. & Sortwell, C.E. (2010a) Stimulation of the rat subthalamic nucleus is neuroprotective following significant nigral dopamine neuron loss. *Neurobiol Dis*, **39**, 105-115.

Spieles-Engemann, A.L., Collier, T.J. & Sortwell, C.E. (2010b) A functionally relevant and long-term model of deep brain stimulation of the rat subthalamic nucleus: advantages and considerations. *The European journal of neuroscience*, **32**, 1092-1099.

Spieles-Engemann, A.L., Steece-Collier, K., Behbehani, M.M., Collier, T.J., Wohlgenant, S.L., Kemp, C.J., Cole-Strauss, A., Levine, N.D., Gombash, S.E., Thompson, V.B., Lipton, J.W. & Sortwell, C.E. (2011) Subthalamic Nucleus Stimulation Increases Brain Derived Neurotrophic Factor in the Nigrostriatal System and Primary Motor Cortex. *Journal of Parkinson's disease*, **1**, 123-136.

Stancak, A., Kozak, J., Vrba, I., Tintera, J., Vrana, J., Polacek, H. & Stancak, M. (2008) Functional magnetic resonance imaging of cerebral activation during spinal cord stimulation in failed back surgery syndrome patients. *Eur J Pain*, **12**, 137-148.

Sun, M., Kong, L., Wang, X., Lu, X.G., Gao, Q. & Geller, A.I. (2005) Comparison of the capability of GDNF, BDNF, or both, to protect nigrostriatal neurons in a rat model of Parkinson's disease. *Brain Res*, **1052**, 119-129.

Thevathasan, W., Mazzone, P., Jha, A., Djamshidian, A., Dileone, M., Di Lazzaro, V. & Brown, P. (2010) Spinal cord stimulation failed to relieve akinesia or restore locomotion in Parkinson disease. *Neurology*, **74**, 1325-1327.

Thomson, E., Lou, J., Sylvester, K., McDonough, A., Tica, S. & Nicolelis, M.A. (2014) Basal forebrain dynamics during a tactile discrimination task. *Journal of neurophysiology*, **112**, 1179-1191.

Thomson, E.E., Carra, R. & Nicolelis, M.A. (2013) Perceiving invisible light through a somatosensory cortical prosthesis. *Nature communications*, **4**, 1482.

Thorn, C.A., Atallah, H., Howe, M. & Graybiel, A.M. (2010) Differential dynamics of activity changes in dorsolateral and dorsomedial striatal loops during learning. *Neuron*, **66**, 781-795.

Tischler, A.S. (1995) Triple immunohistochemical staining for bromodeoxyuridine and catecholamine biosynthetic enzymes using microwave antigen retrieval. *The journal of histochemistry and cytochemistry : official journal of the Histochemistry Society*, **43**, 1-4.

Trimper, J.B., Wolpe, P.R. & Rommelfanger, K.S. (2014) When "I" becomes "We": ethical implications of emerging brain-to-brain interfacing technologies. *Front Neuroeng*, **7**, 4.

van den Brand, R., Heutschi, J., Barraud, Q., DiGiovanna, J., Bartholdi, K., Huerlimann, M., Friedli, L., Vollenweider, I., Moraud, E.M., Duis, S., Dominici, N., Micera, S., Musienko, P. & Courtine, G. (2012) Restoring voluntary control of locomotion after paralyzing spinal cord injury. *Science*, **336**, 1182-1185.

Weber, D.J., Friesen, R. & Miller, L.E. (2012) Interfacing the somatosensory system to restore touch and proprioception: essential considerations. *J Mot Behav*, **44**, 403-418.

Westin, J.E., Janssen, M.L., Sager, T.N. & Temel, Y. (2012) Automated gait analysis in bilateral parkinsonian rats and the role of L-DOPA therapy. *Behav Brain Res*, **226**, 519-528.

Wichmann, T. & DeLong, M.R. (1998) Models of basal ganglia function and pathophysiology of movement disorders. *Neurosurgery clinics of North America*, **9**, 223-236.

Wichmann, T. & Soares, J. (2006) Neuronal firing before and after burst discharges in the monkey basal ganglia is predictably patterned in the normal state and altered in parkinsonism. *Journal of neurophysiology*, **95**, 2120-2133.

Wiest, M.C., Thomson, E., Pantoja, J. & Nicolelis, M.A. (2010) Changes in S1 neural responses during tactile discrimination learning. *Journal of neurophysiology*, **104**, 300-312.

Winkler, C., Kirik, D., Bjorklund, A. & Cenci, M.A. (2002) L-DOPA-induced dyskinesia in the intrastriatal 6-hydroxydopamine model of parkinson's disease: relation to motor and cellular parameters of nigrostriatal function. *Neurobiol Dis*, **10**, 165-186.

Yadav, A.P., Fuentes, R., Zhang, H., Vinholo, T., Wang, C.H., Freire, M.A. & Nicolelis, M.A. (2014) Chronic spinal cord electrical stimulation protects against 6-hydroxydopamine lesions. *Sci Rep*, **4**, 3839.

7. Biography

Amol Prakash Yadav
Born: 25 Aug 1986
Mumbai, Maharashtra, India

Education

PhD, Biomedical Engineering, September 2015
Duke University, Durham, NC

M.S. Biomedical Engineering, May 2010
Duke University, Durham, NC

B.E. Biomedical Engineering, June 2008
University of Mumbai, Mumbai, India

Awards

Masters Tuition Award
Biomedical Engineering, Duke University, 2008

Graduate school Travel Award
Graduate school, Duke University, 2012

Publications

Yadav, A.P., Fuentes, R., Zhang, H., Vinholo, T., Wang, C.H., Freire, M.A. & Nicolelis, M.A. (2014) Chronic spinal cord electrical stimulation protects against 6-hydroxydopamine lesions. *Sci Rep*, **4**, 3839

Pais-Vieira, M., Chiuffa, G., Lebedev, M., **Yadav, A**. & Nicolelis, M.A. (2015) Building an organic computing device with multiple interconnected brains. *Sci Rep*, **5**, 11869

Yadav, A.P., Li, D., Vinholo, T., Lebedev, M., Nicolelis, M.A. A Brainet for Ccortico-Spinal communication (In preparation)

Yadav, A.P., Li, D., Nicolelis, M.A. Artificial Tactile Sensation using Dorsal Column Stimulation (In Preparation)